

Parton coalescence in heavy ion collisions

Gerben Kuipers

Supervisors: Eric Laenen and Thomas Peitzmann

Institute for Theoretical Physics/Institute for Subatomic Physics
Utrecht University

August 2005

Abstract

In the last few years, recombination models have been used to describe hadronization in heavy ion collisions, usually in combination with fragmentation processes. In this thesis we present derivations of the hadron spectra and elliptic flow expressions that are found in the recombination model by Fries *et al.* We conclude that this recombination model correctly predicts an exponential part in the hadron spectra, if the parton phase is assumed to be thermal. Furthermore, we conclude that this model predicts *approximate* quark number scaling of the elliptic flow.

Contents

1	Introduction	4
1.1	Surprises at RHIC	4
1.2	Fragmentation and recombination models	5
2	A homogeneous, static model for coalescing partons	7
2.1	Introduction	7
2.2	Overlap amplitude	7
2.3	Momentum distribution	9
2.4	Approximation	10
2.5	Leading order term	10
2.6	Correction terms	12
2.7	Baryons	13
2.8	Baryon-to-meson ratio	15
2.9	Comparison with fragmentation	16
3	Momentum distributions in the ReCo formalism	18
3.1	Introduction to the formalism	18
3.2	The quantum mechanical density operator	19
3.3	Wigner functions	20
3.4	Lorentz invariance	21
3.5	Simplifications	22
3.6	Using light cone coordinates	23

3.7	Factorized meson Wigner function	25
3.8	Results for narrow longitudinal functions	26
3.9	The hadronization hypersurface	27
3.10	The parton phase	29
3.11	The parton spectrum at zero rapidity	30
3.12	The ReCo meson spectrum at zero rapidity	31
3.13	The ReCo baryon spectrum at zero rapidity	33
4	Elliptic flow	34
4.1	Introduction	34
4.2	Calculation of the parton elliptic flow	38
4.3	Calculation of the meson elliptic flow	39
4.4	Calculation of the baryon elliptic flow	43
4.5	Quark number scaling	47
4.6	Including fragmentation	48
5	A graphic look at the results of the ReCo formalism	49
5.1	Introduction	49
5.2	Momentum distributions	49
5.3	Elliptic flow and quark number scaling	56
6	Conclusions	63
A	Modified Bessel functions	64
A.1	Modified Bessel functions of the first kind	64
A.2	K_1 , a modified Bessel function of the second kind	65

Chapter 1

Introduction

1.1 Surprises at RHIC

In the last few years, many experiments with collisions of large nuclei have been performed at the Relativistic Heavy Ion Collider (RHIC) at Brookhaven National Laboratory in New York State. The hadrons that are produced after a heavy ion collision can provide us with information about the existence of a hot and dense quark-gluon phase called Quark Gluon Plasma: a state of total deconfinement of quarks and gluons. Such a parton phase could exist for a short time after a high energy nucleus-nucleus collision, right before the hadrons are produced from it. In the search for the Quark Gluon Plasma, some very surprising experimental results were found:

- the hadron transverse momentum spectra seem to be built out of an exponential part, followed around 4 – 6 GeV/ c (depending on the hadron species) by a power law tail.
- the measured baryon-to-meson ratios were unusually large: for example, the ratio of protons over positively charged pions is equal or above one for transverse hadron momenta of over 1.5 GeV/ c , and remains approximately constant up to 4 GeV/ c .
- the amount of azimuthal anisotropy in the spectrum of produced hadrons (which is expressed in a quantity called elliptic flow, v_2) depends on the particle species. Moreover, the measured elliptic flows show quark number scaling: the elliptic flows of baryons and mesons are related in a simple way to the elliptic flow of partons, by factors of three and two, respectively (see the almost coinciding pion and proton data in figure 1.1).

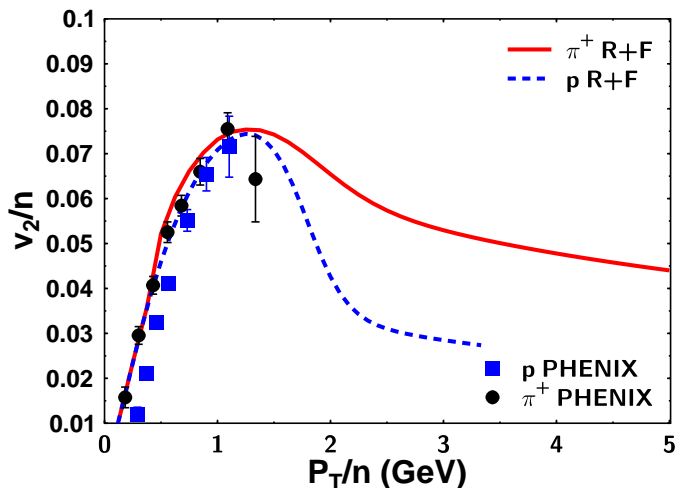


Figure 1.1: Experimental elliptic flow data from PHENIX, divided by 2 for pions (dots) and by 3 for protons (squares), as a function of transverse momentum $P_T/2$ and $P_T/3$, respectively. The solid and dashed lines represent calculations where the recombination model by Fries *et al.* [3] is combined with fragmentation calculations.

1.2 Fragmentation and recombination models

These three experimental facts are striking because they do not fit a description of the hadronization process in terms of *fragmentation*. In a fragmentation picture, perturbative QCD is used to describe how a hadron is formed by a single parton that fragments into a shower of particles containing the meson or baryon that we are interested in. A power law hadron spectrum would be expected, as well as small baryon-to-meson ratios (e.g. a proton-to-pion ratio of about 0.1) and the same elliptic flow values for any hadron species. In a fragmentation process the produced hadron will only have a fraction of the momentum that the fragmenting parton had.

An alternative is to view the hadronization process as a simple recombination process. The basic idea in all recombination (or “ReCo”, or “coalescence”) models is that a hadron is formed not by a fragmenting quark, but by two or three quarks from a hot and dense parton phase (a Quark Gluon Plasma), that are close to each other both in space and in momentum space. Put quite simply, three quarks flying along close to each other coalesce to form a baryon, with a baryon momentum that is the sum of the three parton momenta. Gluons are completely neglected in the description of a recombination process. QCD only plays a background part, to ensure rapid thermalization of the after-collision parton phase, and also to keep the two or three quarks together once they have recombined into a hadron. Since the hadron momentum is now two or three times as high as the momenta of the constituent quarks, the behavior of partons at a certain momentum is translated to comparable hadron behavior at a momentum value that is two or three times as high. This intuitively makes both the measured high baryon-to-meson ratios and the measured scaling of the elliptic flow

more natural.

Even though the basic idea of a recombination process is shared, rather different approaches have been used to turn the basic principle into concrete predictions for the resulting particle spectra (momentum distributions) and elliptic flows. For example, at Texas A&M¹ Monte Carlo implementations (including the effect of resonance decays) of the recombination process were developed, whereas at Duke, Minnesota and Kyoto² mainly analytical methods have been used, assuming a thermal parton distribution. Another difference lies in the way the connection between recombination and fragmentation is treated: the Duke/Minnesota/Kyoto group keeps the behavior of low momentum and high momentum partons strictly separated (only “soft” partons are allowed to recombine and only high momentum partons are allowed to fragment), whereas the Texas group also allows “hard” partons to coalesce.

This thesis follows closely one of the key articles on recombination by the group at Duke, Minnesota and Kyoto (Ref. [3]), providing the reader with detailed and (hopefully) clear derivations of the formulas in the article. In addition to this, we present plots of most of the derived formulas. The main goal of this work is to investigate whether a recombination model can explain the mentioned experimentally observed features in a satisfactory fashion. The emphasis will lie on the treatment and derivation of the momentum dependence of the elliptic flow, but attention is also given to the derivation of hadron momentum distributions. Following the structure of Ref. [3], we will first treat a relatively simple homogeneous and static ReCo model (chapter 2), followed by a more realistic description of coalescing partons (chapters 3, 4 and 5).

¹V. Greco and C. M. Ko [13, 14, 21], among others.

²R. J. Fries, B. Müller, S. A. Bass and C. Nonaka [1, 2, 3].

Chapter 2

A homogeneous, static model for coalescing partons

2.1 Introduction

In this chapter we investigate a very simple (one might say simplistic) model for coalescence: a box of volume V , homogeneously filled with quarks and anti-quarks of one species with a phase space distribution $w(\mathbf{p})$ that does not change during the hadronization process. Thus the quark phase space distribution is not reduced when certain quarks coalesce to form a hadron. Therefore one might call these quarks “quasi-free”. Furthermore, this model does not include any relativistic effects.

It does however describe some of the key features that will interest us in a recombination model: it allows us to calculate the hadron spectra and baryon-to-meson ratio that result from the recombination of thermal quarks. An extensive derivation is presented for mesons, followed by a more concise one for baryons. The question is of course, whether or not this rather crude model can yield realistic physical results. Consequently, we will be mostly interested in the information that can be deduced from leading order terms, and we will approach these results with some caution. But at least we can get our feet wet and see how a recombination process might work.

2.2 Overlap amplitude

To obtain information on coalescence into mesons in our volume, we have to calculate the overlap between a two-parton state and a meson state. The spatial wave function $\psi(\mathbf{x}_1, \mathbf{x}_2)$ for a two particle quark/antiquark state with momenta \mathbf{p}_1 and \mathbf{p}_2 can be derived from the

Schrödinger equation to be (see for example Ref. [5])

$$\langle \mathbf{x}_1, \mathbf{x}_2 | \mathcal{Q} \mathbf{p}_1 \mathbf{p}_2 \rangle = V^{-1} e^{i(\mathbf{p}_1 \cdot \mathbf{x}_1 + \mathbf{p}_2 \cdot \mathbf{x}_2)}, \quad (2.2.1)$$

in which \mathcal{Q} stands for “quark”. This wave function is easily seen to satisfy the normalization requirement $\int d^3x_1 d^3x_2 |\psi(\mathbf{x}_1, \mathbf{x}_2)|^2 = 1$. For a meson of type M (consisting of a quark and an anti-quark in a bound state with momentum \mathbf{P}), the spatial wave function is

$$\langle \mathbf{x}_1, \mathbf{x}_2 | M \mathbf{P} \rangle = V^{-\frac{1}{2}} e^{i\mathbf{P} \cdot \mathbf{R}} \varphi_M(\mathbf{y}), \quad (2.2.2)$$

where $\mathbf{R} = (\mathbf{x}_1 + \mathbf{x}_2)/2$ is the centre of mass coordinate, and $\mathbf{y} = \mathbf{x}_1 - \mathbf{x}_2$ is the relative coordinate. The wave function φ_M describes the “internal” physics of the meson, and therefore depends on the relative coordinate \mathbf{y} . Demanding the meson wave function (2.2.2) to be normalized leads to the following requirement for φ_M :

$$\int d^3y |\varphi_M(\mathbf{y})|^2 = 1. \quad (2.2.3)$$

Now we can calculate the squared overlap amplitude by making use of expressions (2.2.1) and (2.2.2), and the definitions of \mathbf{R} and \mathbf{y} in terms of \mathbf{x}_1 and \mathbf{x}_2 :

$$\begin{aligned} |\langle \mathcal{Q} \mathbf{p}_1 \mathbf{p}_2 | M \mathbf{P} \rangle|^2 &= \left| \int d^3x_1 d^3x_2 \langle \mathcal{Q} \mathbf{p}_1 \mathbf{p}_2 | \mathbf{x}_1, \mathbf{x}_2 \rangle \langle \mathbf{x}_1, \mathbf{x}_2 | M \mathbf{P} \rangle \right|^2 \\ &= \left| V^{-3/2} \int d^3x_1 d^3x_2 e^{i(\mathbf{P}/2 - \mathbf{p}_1) \cdot \mathbf{x}_1} e^{i(\mathbf{P}/2 - \mathbf{p}_2) \cdot \mathbf{x}_2} \varphi_M(\mathbf{x}_1 - \mathbf{x}_2) \right|^2 \\ &= \left| V^{-3/2} \int d^3x_1 d^3x_2 e^{i(\mathbf{P}/2 - \mathbf{p}_1) \cdot \mathbf{x}_1} e^{i(\mathbf{P}/2 - \mathbf{p}_2) \cdot \mathbf{x}_2} \left(\int \frac{d^3k}{(2\pi)^3} \hat{\varphi}_M(\mathbf{k}) e^{i\mathbf{k} \cdot (\mathbf{x}_1 - \mathbf{x}_2)} \right) \right|^2 \\ &= \left| V^{-3/2} \int \frac{d^3k}{(2\pi)^3} \left(\int d^3x_1 e^{i(\mathbf{P}/2 - \mathbf{p}_1 + \mathbf{k}) \cdot \mathbf{x}_1} \right) \left(\int d^3x_2 e^{i(\mathbf{P}/2 - \mathbf{p}_2 - \mathbf{k}) \cdot \mathbf{x}_2} \right) \hat{\varphi}_M(\mathbf{k}) \right|^2 \\ &= \left| V^{-3/2} \int \frac{d^3k}{(2\pi)^3} ((2\pi)^3 \delta^{(3)}(\mathbf{P}/2 - \mathbf{p}_1 + \mathbf{k})) ((2\pi)^3 \delta^{(3)}(\mathbf{P}/2 - \mathbf{p}_2 - \mathbf{k})) \hat{\varphi}_M(\mathbf{k}) \right|^2 \\ &= \frac{(2\pi)^6}{V^3} \left| \delta^{(3)}(\mathbf{P} - \mathbf{p}_1 - \mathbf{p}_2) \hat{\varphi}_M((\mathbf{p}_1 - \mathbf{p}_2)/2) \right|^2, \end{aligned} \quad (2.2.4)$$

with $\hat{\varphi}_M$ the Fourier transform of φ_M , using the convention $\varphi_M(x) = (2\pi)^{-3} \int d^3k \hat{\varphi}_M(k) e^{i\mathbf{k} \cdot \mathbf{x}}$. Note that we are using Fourier transformations and Dirac delta functions as if the momenta are continuous and space is unbounded. In fact we started this chapter by saying that we are looking at a boxed world, of volume V . Demanding the wave function to still be single-valued in a bounded space immediately leads to quantization of the momenta. Therefore, we should really have used Kronecker deltas instead of Dirac delta functions. That is, we should really change

$$\delta^{(3)}(\mathbf{p}) \rightarrow \frac{V}{(2\pi)^3} \delta_{\mathbf{p}}. \quad (2.2.5)$$

But since Dirac delta functions are generally a little more convenient for our purposes, we will continue to use them anyway, as well as integrations instead of summations over momenta. However, now that we are faced with an expression containing the absolute value squared of a delta function, we need to realize what this means in terms of Kronecker deltas:

$$\left| \frac{V}{(2\pi)^3} \delta_{\mathbf{p}} \right|^2 = \left(\frac{V}{(2\pi)^3} \right)^2 \delta_{\mathbf{p}}^2 = \left(\frac{V}{(2\pi)^3} \right)^2 \delta_{\mathbf{p}} = \frac{V}{(2\pi)^3} \left(\frac{V}{(2\pi)^3} \delta_{\mathbf{p}} \right). \quad (2.2.6)$$

Therefore, we write

$$|\delta^{(3)}(\mathbf{p})|^2 = \frac{V}{(2\pi)^3} \delta^{(3)}(\mathbf{p}). \quad (2.2.7)$$

With this our squared overlap amplitude simplifies to

$$|\langle \mathcal{Q} \mathbf{p}_1 \mathbf{p}_2 | M \mathbf{P} \rangle|^2 = \frac{(2\pi)^3}{V^2} \delta^{(3)}(\mathbf{P} - \mathbf{p}_1 - \mathbf{p}_2) |\hat{\varphi}_M(\mathbf{q})|^2, \quad (2.2.8)$$

where $\mathbf{q} = (\mathbf{p}_1 - \mathbf{p}_2)/2$ is the relative momentum of the two quarks.

2.3 Momentum distribution

The total number of mesons of type M that are formed by coalescing partons in our volume V is related to the individual phase space densities of the partons and to the squared overlap amplitude by

$$N_M = C_M V^3 \int \frac{d^3 P}{(2\pi)^3} \frac{d^3 p_1}{(2\pi)^3} \frac{d^3 p_2}{(2\pi)^3} w(\mathbf{p}_1) w(\mathbf{p}_2) |\langle \mathcal{Q} \mathbf{p}_1 \mathbf{p}_2 | M \mathbf{P} \rangle|^2, \quad (2.3.1)$$

where the three factors of V arise from three integrations over space involving a space-independent integrand. C_M is the degeneracy factor of the meson of type M . It counts the number of ways in which a meson of type M can be made out of quarks with different quantum numbers. For example, for the pion we simply have $C_\pi = 1$.

To obtain the momentum distribution for mesons, we write (2.3.1) as

$$\frac{dN_M}{d^3 P} = C_M \frac{V^3}{(2\pi)^3} \int \frac{d^3 p_1}{(2\pi)^3} \frac{d^3 p_2}{(2\pi)^3} w(\mathbf{p}_1) w(\mathbf{p}_2) |\langle \mathcal{Q} \mathbf{p}_1 \mathbf{p}_2 | M \mathbf{P} \rangle|^2. \quad (2.3.2)$$

Now we can plug in the squared overlap amplitude (2.2.8):

$$\frac{dN_M}{d^3 P} = C_M \frac{V}{(2\pi)^3} \int \frac{d^3 p_1}{(2\pi)^3} d^3 p_2 w(\mathbf{p}_1) w(\mathbf{p}_2) \delta^{(3)}(\mathbf{P} - \mathbf{p}_1 - \mathbf{p}_2) |\hat{\varphi}_M((\mathbf{p}_1 - \mathbf{p}_2)/2)|^2. \quad (2.3.3)$$

To work this out, first we perform a substitution of variables from \mathbf{p}_1 to the same relative momentum \mathbf{q} we used in (2.2.8) by writing $\mathbf{p}_1 = 2\mathbf{q} + \mathbf{p}_2$:

$$\frac{dN_M}{d^3 P} = C_M \frac{V}{(2\pi)^3} \int \frac{2d^3 q}{(2\pi)^3} d^3 p_2 w(2\mathbf{q} + \mathbf{p}_2) w(\mathbf{p}_2) \delta^{(3)}(\mathbf{P} - (2\mathbf{q} + \mathbf{p}_2) - \mathbf{p}_2) |\hat{\varphi}_M(\mathbf{q})|^2$$

$$= C_M \frac{V}{(2\pi)^3} \int \frac{d^3q}{(2\pi)^3} d^3p_2 w(2\mathbf{q} + \mathbf{p}_2) w(\mathbf{p}_2) 2 \delta^{(3)}\left(2\left(\frac{\mathbf{P}}{2} - \mathbf{q} - \mathbf{p}_2\right)\right) |\hat{\varphi}_M(\mathbf{q})|^2. \quad (2.3.4)$$

We can perform the integral over \mathbf{p}_2 , using $2\delta(2x) = \delta(x)$, to obtain

$$\frac{dN_M}{d^3P} = C_M \frac{V}{(2\pi)^3} \int \frac{d^3q}{(2\pi)^3} w\left(\frac{\mathbf{P}}{2} + \mathbf{q}\right) w\left(\frac{\mathbf{P}}{2} - \mathbf{q}\right) |\hat{\varphi}_M(\mathbf{q})|^2. \quad (2.3.5)$$

2.4 Approximation

We assume that the absolute value of the wave function $\hat{\varphi}_M$ drops rapidly and approaches zero when q (by which I mean $\|\mathbf{q}\|$) becomes larger than a certain width Λ_M . This simply means that the probability of finding values of the relative momentum of the two partons that are larger than Λ_M , is very small. As a result of this assumption, the integral over \mathbf{q} in (2.3.5) will be dominated by contributions where q is of the order of Λ_M or smaller. We are interested in the momentum distribution for large meson momenta, at least much larger than Λ_M . But then q is much smaller than P in relevant contributions to the integral in (2.3.5). Therefore we can approximate both phase space distributions in this integrand by Taylor expansions up to second order:

$$w\left(\frac{\mathbf{P}}{2} + \mathbf{q}\right) = w\left(\frac{\mathbf{P}}{2}\right) + \sum_{i=1}^3 q_i \partial_i w\left(\frac{\mathbf{P}}{2}\right) + \frac{1}{2} \sum_{i,j=1}^3 q_i q_j \partial_i \partial_j w\left(\frac{\mathbf{P}}{2}\right) + \mathcal{O}(q^3), \quad (2.4.1)$$

and

$$w\left(\frac{\mathbf{P}}{2} - \mathbf{q}\right) = w\left(\frac{\mathbf{P}}{2}\right) - \sum_{i=1}^3 q_i \partial_i w\left(\frac{\mathbf{P}}{2}\right) + \frac{1}{2} \sum_{i,j=1}^3 q_i q_j \partial_i \partial_j w\left(\frac{\mathbf{P}}{2}\right) + \mathcal{O}(q^3). \quad (2.4.2)$$

It is easy to see that in the product of these two expansions the terms of first order in q cancel each other. We are left with a zeroth order term and a second order term:

$$w\left(\frac{\mathbf{P}}{2} + \mathbf{q}\right) w\left(\frac{\mathbf{P}}{2} - \mathbf{q}\right) = w\left(\frac{\mathbf{P}}{2}\right)^2 + \sum_{i,j=1}^3 q_i q_j \left[w\left(\frac{\mathbf{P}}{2}\right) \partial_i \partial_j w\left(\frac{\mathbf{P}}{2}\right) - \partial_i w\left(\frac{\mathbf{P}}{2}\right) \partial_j w\left(\frac{\mathbf{P}}{2}\right) \right] + \mathcal{O}(q^3). \quad (2.4.3)$$

2.5 Leading order term

The lowest order term in (2.4.3) is a constant with regard to \mathbf{q} . We can immediately plug it into our expression for the meson momentum distribution (2.3.5) and calculate the result.

We only need to perform a Fourier transformation to make connection with the normalization requirement (2.2.3):

$$\begin{aligned}
\left(\frac{dN_M}{d^3P}\right)_{\text{leading order}} &= C_M \frac{V}{(2\pi)^3} \int \frac{d^3q}{(2\pi)^3} w\left(\frac{\mathbf{P}}{2}\right)^2 |\hat{\varphi}_M(\mathbf{q})|^2 \\
&= C_M \frac{V}{(2\pi)^3} w\left(\frac{\mathbf{P}}{2}\right)^2 \int \frac{d^3q}{(2\pi)^3} \left(\int d^3y \varphi_M^*(\mathbf{y}) e^{i\mathbf{q}\cdot\mathbf{y}} \right) \left(\int d^3z \varphi_M(\mathbf{z}) e^{-i\mathbf{q}\cdot\mathbf{z}} \right) \\
&= C_M \frac{V}{(2\pi)^3} w\left(\frac{\mathbf{P}}{2}\right)^2 \frac{1}{(2\pi)^3} \int d^3y \int d^3z (2\pi)^3 \delta^{(3)}(\mathbf{z}-\mathbf{y}) \varphi_M^*(\mathbf{y}) \varphi_M(\mathbf{z}) \\
&= C_M \frac{V}{(2\pi)^3} w\left(\frac{\mathbf{P}}{2}\right)^2 \int d^3y |\varphi_M(\mathbf{y})|^2 = C_M \frac{V}{(2\pi)^3} w\left(\frac{\mathbf{P}}{2}\right)^2. \quad (2.5.1)
\end{aligned}$$

Note that the only assumption regarding φ_M we have had to make to arrive at this result, is that its absolute value drops rapidly for values of q larger than Λ_M . No other knowledge of φ_M was needed. However, if we plug the q -dependent second order term from the Taylor expansion into (2.3.5), we *will* have to use an expression for $\hat{\varphi}_M$. Of course we want a function that shows the behavior mentioned in section 2.4. Therefore, we choose a Gaussian shape with a width Λ_M . In formula, with the appropriate normalization constant to suit (2.2.3),

$$\hat{\varphi}_M(\mathbf{q}) = \mathcal{N}_M e^{-q^2/2\Lambda_M^2} = \left(\frac{2\sqrt{\pi}}{\Lambda_M}\right)^{3/2} e^{-q^2/2\Lambda_M^2}. \quad (2.5.2)$$

We take a thermal parton phase space distribution

$$w(\mathbf{p}) = \mathcal{A} e^{-p/T} = \frac{\pi^2}{T^3} \left(\frac{N_Q}{V}\right) e^{-p/T}, \quad (2.5.3)$$

with N_Q the total number of quarks in the volume V . This normalization is such that, if we integrate the phase space distribution over both coordinate space and momentum space, we get the total number of quarks in the volume:

$$V \int \frac{d^3p}{(2\pi)^3} w(\mathbf{p}) = N_Q. \quad (2.5.4)$$

However, it must be emphasized that in this simple model the interactions that in reality will exist between partons are not taken into account: we are dealing with a volume filled with a fixed number of quarks and anti-quarks. In our description no extra partons are produced when the temperature parameter increases. So, whereas normally one would expect the number of partons N_Q to be proportional to T^3 (see for example Ref. [6], p. 166), in this simple model we take N_Q to be a fixed number. As a result, the temperature parameter in the derived formulas should not be taken too seriously. In our model it simply plays the part of a scale for the momentum of the considered particles.

With expression (2.5.3) for $w(\mathbf{p})$, the leading term of the meson momentum distribution (2.5.1) becomes

$$\left(\frac{dN_M}{d^3P}\right)_{\text{leading order}} = C_M \mathcal{A}^2 \frac{V}{(2\pi)^3} e^{-P/T} = \frac{\pi}{8} \frac{C_M N_Q^2}{T^6 V} e^{-P/T}. \quad (2.5.5)$$

2.6 Correction terms

Now we want to calculate the correction to (2.5.5), resulting from the rather large second order term in the Taylor expansion (2.4.3). Let us first look at the terms in which $i \neq j$. For these, using the product rule, it is easy to calculate that

$$\partial_i \partial_j w(\mathbf{p}) = \mathcal{A} \frac{p_i p_j}{p^2 T} \left(\frac{1}{p} + \frac{1}{T} \right) e^{-p/T}. \quad (2.6.1)$$

Multiplying with $w(\mathbf{p})$ and subsequently replacing \mathbf{p} with $\mathbf{P}/2$, we find

$$w(\mathbf{P}/2) \partial_i \partial_j w(\mathbf{P}/2) = \mathcal{A}^2 \frac{P_i P_j}{P^2 T} \left(\frac{2}{P} + \frac{1}{T} \right) e^{-P/T}. \quad (2.6.2)$$

Similarly, we calculate (also for $i \neq j$)

$$\partial_i w(\mathbf{P}/2) \partial_j w(\mathbf{P}/2) = \mathcal{A}^2 \frac{P_i P_j}{P^2 T^2} e^{-P/T}. \quad (2.6.3)$$

Now let us look at the case $i = j$. We use again the product rule to find

$$w(\mathbf{P}/2) \partial_i \partial_i w(\mathbf{P}/2) = \mathcal{A}^2 \left(-\frac{2}{PT} + \frac{2P_i^2}{P^3 T} + \frac{P_i^2}{P^2 T^2} \right) e^{-P/T}, \quad (2.6.4)$$

where no summation convention is intended. In the same way,

$$\partial_i w(\mathbf{P}/2) \partial_i w(\mathbf{P}/2) = \mathcal{A}^2 \frac{P_i^2}{P^2 T^2} e^{-P/T}. \quad (2.6.5)$$

Now we have all that we need to write out the total second order term of our Taylor expansion (2.4.3). Simply gathering terms and using the definition of the dot product, we can write

$$\begin{aligned} \sum_{i,j=1}^3 q_i q_j \left[w\left(\frac{\mathbf{P}}{2}\right) \partial_i \partial_j w\left(\frac{\mathbf{P}}{2}\right) - \partial_i w\left(\frac{\mathbf{P}}{2}\right) \partial_j w\left(\frac{\mathbf{P}}{2}\right) \right] &= 2\mathcal{A}^2 \sum_{i \neq j} \left(q_i q_j \frac{P_i P_j}{P^3 T} \right) e^{-P/T} \\ + \mathcal{A}^2 \sum_i q_i^2 \left(-\frac{2}{PT} + \frac{2P_i^2}{P^3 T} \right) e^{-P/T} &= 2\mathcal{A}^2 \sum_{i,j} \left(\frac{q_i P_i q_j P_j}{P^3 T} \right) e^{-P/T} - \mathcal{A}^2 \frac{2}{PT} q^2 e^{-P/T} \\ &= 2\mathcal{A}^2 \frac{(\mathbf{q} \cdot \mathbf{P})^2}{P^3 T} e^{-P/T} - 2\mathcal{A}^2 \frac{q^2}{PT} e^{-P/T}. \end{aligned} \quad (2.6.6)$$

If we plug the first term of (2.6.6), together with the Gaussian internal wave function (2.5.2), into the momentum distribution expression (2.3.5), we get¹

$$\begin{aligned}
\left(\frac{dN_M}{d^3P}\right)_{\text{correction 1}} &= 2 C_M \mathcal{A}^2 \frac{V}{(2\pi)^3} \int \frac{d^3q}{(2\pi)^3} \frac{(\mathbf{q} \cdot \mathbf{P})^2}{P^3 T} e^{-P/T} \mathcal{N}_M^2 e^{-q^2/\Lambda_M^2} \\
&= 2 C_M \mathcal{N}_M^2 \mathcal{A}^2 \frac{V}{(2\pi)^3} \frac{e^{-P/T}}{(2\pi)^3} 2\pi \int_0^\infty q^2 dq \int_0^\pi \sin \theta d\theta \frac{(q^2 P^2 \cos^2 \theta)}{P^3 T} e^{-q^2/\Lambda_M^2} \\
&= 2 C_M \mathcal{N}_M^2 \mathcal{A}^2 \frac{V}{(2\pi)^3} \frac{e^{-P/T}}{(2\pi)^3 P T} \cdot 2\pi \cdot \frac{2}{3} \cdot \int_0^\infty dq q^4 e^{-q^2/\Lambda_M^2} \\
&= 2 C_M \mathcal{N}_M^2 \mathcal{A}^2 \frac{V}{(2\pi)^3} \frac{e^{-P/T}}{(2\pi)^3 P T} \cdot 2\pi \cdot \frac{2}{3} \cdot \left(\frac{3}{8} \sqrt{\pi} \Lambda_M^5\right) = C_M \mathcal{A}^2 \frac{V}{(2\pi)^3} \frac{e^{-P/T}}{P T} \Lambda_M^2. \quad (2.6.7)
\end{aligned}$$

From the second term in (2.6.6) we get

$$\begin{aligned}
\left(\frac{dN_M}{d^3P}\right)_{\text{correction 2}} &= -2 C_M \mathcal{A}^2 \frac{V}{(2\pi)^3} \int \frac{d^3q}{(2\pi)^3} \cdot \frac{q^2}{P T} e^{-P/T} \mathcal{N}_M^2 e^{-q^2/\Lambda_M^2} \\
&= -2 C_M \mathcal{N}_M^2 \mathcal{A}^2 \frac{V}{(2\pi)^3} \frac{e^{-P/T}}{(2\pi)^3 P T} 4\pi \int_0^\infty dq q^4 e^{-q^2/\Lambda_M^2} \\
&= -2 C_M \mathcal{N}_M^2 \mathcal{A}^2 \frac{V}{(2\pi)^3} \frac{e^{-P/T}}{(2\pi)^3 P T} \cdot 4\pi \cdot \left(\frac{3}{8} \sqrt{\pi} \Lambda_M^5\right) = -3 C_M \mathcal{A}^2 \frac{V}{(2\pi)^3} \frac{e^{-P/T}}{P T} \Lambda_M^2. \quad (2.6.8)
\end{aligned}$$

Adding (2.6.7) and (2.6.8), we find the total second-order correction to the leading order term (2.5.5) to be

$$\left(\frac{dN_M}{d^3P}\right)_{\text{correction}} = -2 C_M \mathcal{A}^2 \frac{V}{(2\pi)^3} \frac{e^{-P/T}}{P T} \Lambda_M^2. \quad (2.6.9)$$

So, including this correction, the expression for the meson momentum distribution finally becomes

$$\frac{dN_M}{d^3P} = C_M \mathcal{A}^2 \frac{V}{(2\pi)^3} e^{-P/T} \left[1 - \frac{2\Lambda_M^2}{T P}\right] = \frac{\pi}{8} \frac{C_M N_Q^2}{T^6 V} e^{-P/T} \left[1 - \frac{2\Lambda_M^2}{T P}\right]. \quad (2.6.10)$$

2.7 Baryons

For baryons the derivation of the momentum distribution is analogous to the derivation presented above. However, there are a couple of subtle differences. The wave functions are

$$\langle \mathbf{x}_1, \mathbf{x}_2, \mathbf{x}_3 \mid \mathcal{Q} \mathbf{p}_1, \mathbf{p}_2, \mathbf{p}_3 \rangle = V^{-3/2} e^{i(\mathbf{p}_1 \cdot \mathbf{x}_1 + \mathbf{p}_2 \cdot \mathbf{x}_2 + \mathbf{p}_3 \cdot \mathbf{x}_3)} \quad (2.7.1)$$

¹Here I use the following integrals: $\int_0^\pi d\theta \sin \theta \cos^2 \theta = \frac{2}{3}$ and $\int_0^\infty dq q^4 e^{-aq^2} = \frac{3}{8} \sqrt{\frac{\pi}{a^5}}$.

for the three particle state, and

$$\langle \mathbf{x}_1, \mathbf{x}_2, \mathbf{x}_3 | B \mathbf{P} \rangle = V^{-1/2} e^{i\mathbf{P}\cdot\mathbf{R}} \varphi_B(\mathbf{y}, \mathbf{z}) \quad (2.7.2)$$

for the baryon state with momentum \mathbf{P} . Clearly, we now need not one but *two* relative coordinates: $\mathbf{y} = (\mathbf{x}_1 + \mathbf{x}_2)/2 - \mathbf{x}_3$ and $\mathbf{z} = \mathbf{x}_1 - \mathbf{x}_2$. Consequently, there are also two associated relative momenta, \mathbf{q} and \mathbf{s} .

Using the same tools as in the derivation of (2.2.8) (i.e., plugging in a completeness relation and Fourier transforming φ_B) the squared overlap amplitude is found to be

$$\begin{aligned} |\langle \mathcal{Q} \mathbf{p}_1, \mathbf{p}_2, \mathbf{p}_3 | B \mathbf{P} \rangle|^2 &= \left| \frac{(2\pi)^3}{V^2} \delta^{(3)}(\mathbf{P} - \mathbf{p}_1 - \mathbf{p}_2 - \mathbf{p}_3) \hat{\varphi}_B(\mathbf{q}, \mathbf{s}) \right|^2 \\ &= \frac{(2\pi)^3}{V^3} \delta^{(3)}(\mathbf{P} - \mathbf{p}_1 - \mathbf{p}_2 - \mathbf{p}_3) |\hat{\varphi}_B(\mathbf{q}, \mathbf{s})|^2, \end{aligned} \quad (2.7.3)$$

in which the relative momenta \mathbf{q} and \mathbf{s} turn out to be

$$\mathbf{q} = \frac{2}{3} \left(\frac{\mathbf{p}_1 + \mathbf{p}_2}{2} - \mathbf{p}_3 \right) \quad (2.7.4)$$

and

$$\mathbf{s} = \frac{\mathbf{p}_1 - \mathbf{p}_2}{2}. \quad (2.7.5)$$

The total number of baryons of type B is related to the individual phase space densities of the partons and to the squared overlap amplitude by

$$N_B = C_B V^4 \int \frac{d^3P}{(2\pi)^3} \frac{d^3p_1}{(2\pi)^3} \frac{d^3p_2}{(2\pi)^3} \frac{d^3p_3}{(2\pi)^3} w(\mathbf{p}_1)w(\mathbf{p}_2)w(\mathbf{p}_3) |\langle \mathcal{Q} \mathbf{p}_1, \mathbf{p}_2, \mathbf{p}_3 | B \mathbf{P} \rangle|^2, \quad (2.7.6)$$

so the momentum distribution reads

$$\begin{aligned} \frac{dN_B}{d^3P} &= C_B \frac{V}{(2\pi)^3} \int \frac{d^3p_1}{(2\pi)^3} \frac{d^3p_2}{(2\pi)^3} d^3p_3 w(\mathbf{p}_1)w(\mathbf{p}_2)w(\mathbf{p}_3) \delta^{(3)}(\mathbf{P} - \mathbf{p}_1 - \mathbf{p}_2 - \mathbf{p}_3) |\hat{\varphi}_B(\mathbf{q}, \mathbf{s})|^2 \\ &= C_B \frac{V}{(2\pi)^3} \int \frac{d^3q}{(2\pi)^3} \frac{d^3s}{(2\pi)^3} w\left(\frac{\mathbf{P}}{3} + \frac{\mathbf{q}}{2} + \mathbf{s}\right) w\left(\frac{\mathbf{P}}{3} + \frac{\mathbf{q}}{2} - \mathbf{s}\right) w\left(\frac{\mathbf{P}}{3} - \mathbf{q}\right) |\hat{\varphi}_B(\mathbf{q}, \mathbf{s})|^2. \end{aligned} \quad (2.7.7)$$

Assuming again that $|\hat{\varphi}_B(\mathbf{q}, \mathbf{s})|^2$ rapidly approaches zero when q or s becomes large, we can make a Taylor approximation of the product of parton phase space distributions in both q and s . The leading term of this approximation will be $w(\mathbf{P}/3)^3$, so the leading term of the baryon momentum distribution will be

$$\left(\frac{dN_B}{d^3P} \right)_{\text{leading order}} = C_B \frac{V}{(2\pi)^3} w\left(\frac{\mathbf{P}}{3}\right)^3. \quad (2.7.8)$$

With the thermal parton phase space distribution (2.5.3) this becomes

$$\left(\frac{dN_B}{d^3P}\right)_{\text{leading order}} = C_B \mathcal{A}^3 \frac{V}{(2\pi)^3} e^{-P/T} = C_B \frac{\pi^3}{8} \frac{N_Q^3}{T^9 V^2} e^{-P/T}. \quad (2.7.9)$$

As in the previous subsection, corrections to this result can be calculated from higher order terms of the Taylor expansion. In such calculations, the internal wave function can be assumed to be a Gaussian, both with respect to \mathbf{q} and with respect to \mathbf{s} :

$$\hat{\varphi}_B(\mathbf{q}, \mathbf{s}) = \mathcal{N}_B e^{-q^2/2\Lambda_{B,1}^2} e^{-s^2/2\Lambda_{B,2}^2} = \left(\frac{4\pi}{\Lambda_{B,1}\Lambda_{B,2}}\right)^{3/2} e^{-q^2/2\Lambda_{B,1}^2} e^{-s^2/2\Lambda_{B,2}^2}. \quad (2.7.10)$$

2.8 Baryon-to-meson ratio

It is immediately seen, by comparing (2.5.5) and (2.7.9), that in this model for coalescence the baryon-to-meson ratio is in leading order independent of hadron momentum. The ratio only depends on the temperature parameter T , on the parton density in our volume, and on the degeneracy factors:

$$\frac{dN_B}{dN_M} = \frac{C_B \frac{V}{(2\pi)^3} \mathcal{A}^3 e^{-P/T}}{C_M \frac{V}{(2\pi)^3} \mathcal{A}^2 e^{-P/T}} = \mathcal{A} \frac{C_B}{C_M} = \frac{\pi^2}{T^3} \left(\frac{N_Q}{V}\right) \frac{C_B}{C_M}. \quad (2.8.1)$$

We can use this expression to estimate the ReCo proton-to-pion ratio in this model:

$$\frac{dN_p}{dN_\pi} = \frac{\pi^2}{T^3} \left(\frac{N_Q}{V}\right) \frac{C_p}{C_\pi}. \quad (2.8.2)$$

Taking $C_p = 2$, $C_\pi = 1$, $T = 175$ MeV and $N_Q/V = 3 \text{ fm}^{-3}$, we would get an absurdly high proton-to-pion ratio of 86. This value is not in accordance with experimental results from the PHENIX collaboration [4] (it should be of the order of 1). Our unrealistic result is caused by the fact that the normalization constant $\mathcal{A} = (\pi^2/T^3)(N_Q/V)$ does not drop out in the baryon-to-meson ratio.

Note that the striking independence of the hadron momentum arises only when we assume a thermal (exponential) parton phase space distribution. If in fact we have a power law parton spectrum,

$$w(\mathbf{p}) = A \left(\frac{p}{\mu}\right)^{-\alpha}, \quad (2.8.3)$$

then the coalescence baryon-to-meson ratio will still depend on the hadron momentum, even if we still only use the leading order terms of the momentum distributions:

$$\frac{dN_B}{dN_M} = \frac{C_B \frac{V}{(2\pi)^3} A^3 (P/3\mu)^{-3\alpha}}{C_M \frac{V}{(2\pi)^3} A^2 (P/2\mu)^{-2\alpha}} = A \frac{C_B}{C_M} \left(\frac{4P}{9\mu}\right)^{-\alpha}. \quad (2.8.4)$$

2.9 Comparison with fragmentation

2.9.1 Fragmentation functions

If the formation of hadrons of type H in our volume would be governed by the process of fragmentation instead of by coalescence, we would have the hadron momentum distribution

$$\frac{dN_H}{d^3P} = \frac{V}{(2\pi)^3} \int_0^1 \frac{dz}{z^3} D_{Q \rightarrow H}(z) w\left(\frac{\mathbf{P}}{z}\right). \quad (2.9.1)$$

In this formula, $D_{Q \rightarrow H}(z)$ represents the probability for a hadron of type H and with momentum $\mathbf{P} = z\mathbf{p}$ to result from a fragmenting quark with momentum \mathbf{p} . Therefore, $D_{Q \rightarrow H}(z)$ is usually referred to as a ‘‘fragmentation function’’. Fragmentation functions can be determined from experiments (for example, see Ref. [7]). A commonly used parametrization of the fragmentation function (which is also used in Ref. [7]) is

$$D_{Q \rightarrow H}(z) = Nz^\alpha(1-z)^\beta, \quad (2.9.2)$$

where values of N , α and β depend on the type of quark that is fragmenting and of course on the type of meson or baryon that one is interested in.

For our purposes however, it will suffice to approximate expression (2.9.1), using a thermal parton phase space distribution, by

$$\frac{V}{(2\pi)^3} \mathcal{A} \langle D_H \rangle e^{-P/\langle z \rangle T}, \quad (2.9.3)$$

with the average values $\langle D_H \rangle$ and $\langle z \rangle$ both between 0 and 1.

2.9.2 Mesons from a thermal parton spectrum

Using approximation (2.9.3), and taking only the leading order term of the coalescence momentum distribution (2.6.10) into account, we can estimate that for mesons of type M

$$\frac{\text{coalescence}}{\text{fragmentation}} = \frac{\mathcal{A}^2}{\mathcal{A}} \frac{C_M}{\langle D_M \rangle} e^{-\frac{P}{T}(1-\frac{1}{\langle z \rangle})} = \frac{\pi^2}{T^3} \left(\frac{N_Q}{V} \right) \frac{C_M}{\langle D_M \rangle} e^{\frac{P}{T}(\frac{1}{\langle z \rangle}-1)}. \quad (2.9.4)$$

Note that the average value of z is smaller than 1, so the exponent is positive. Given this exponential shape, one would expect that coalescence would become the dominant meson production mechanism for mesons with large momenta, as soon as the ratio becomes bigger than 1, whereas for small meson momenta fragmentation would dominate. The ratio equals 1 when

$$P = - \frac{T \log \left(\frac{\pi^2}{T^3} \left(\frac{N_Q}{V} \right) \frac{C_M}{\langle D_M \rangle} \right)}{\frac{1}{\langle z \rangle} - 1}. \quad (2.9.5)$$

But it is easily seen that the value of this “crossover” hadron momentum is negative, since with realistic values for the temperature and the parton density, we find $\frac{\pi^2}{T^3} \left(\frac{N_Q}{V}\right) \frac{C_M}{\langle D_M \rangle} > 1$. We can conclude that, in this model, coalescence dominates as the mechanism for producing mesons, for every (positive) value of the meson momentum.

2.9.3 Baryons from a thermal parton spectrum

We can make a similar coalescence-fragmentation comparison for baryons. Here the dependence on parton density is even stronger, because there are *three* factors of the parton phase space density in the baryon momentum distribution (2.7.8), and still only one factor of w in the fragmentation formula (2.9.1). Thus, the baryon coalescence-to-fragmentation ratio is

$$\frac{\text{coalescence}}{\text{fragmentation}} = \frac{\mathcal{A}^3 C_B}{\mathcal{A} \langle D_B \rangle} e^{-\frac{P}{T}(1-\frac{1}{\langle z \rangle})} = \left[\frac{\pi^2}{T^3} \left(\frac{N_Q}{V} \right) \right]^2 \frac{C_B}{\langle D_B \rangle} e^{-\frac{P}{T}(1-\frac{1}{\langle z \rangle})}, \quad (2.9.6)$$

and the transition momentum where coalescence takes over from fragmentation is

$$P = - \frac{T \log \left(\left[\frac{\pi^2}{T^3} \left(\frac{N_Q}{V} \right) \right]^2 \frac{C_B}{\langle D_B \rangle} \right)}{\frac{1}{\langle z \rangle} - 1}. \quad (2.9.7)$$

This is again a negative number, so in this model recombination would dominate also for baryons of any momentum.

2.9.4 Power law parton distribution

On the other hand, for a parton spectrum of the form $w(\mathbf{p}) = A(p/\mu)^{-\alpha}$ with $\alpha > 0$, we find the meson coalescence-to-fragmentation ratio

$$\frac{\text{coalescence}}{\text{fragmentation}} = \frac{C_M A}{\langle D \rangle} \left(\frac{4}{\langle z \rangle} \right)^\alpha \left(\frac{P}{\mu} \right)^{-\alpha}. \quad (2.9.8)$$

Clearly, in this case fragmentation will dominate as a production mechanism for large meson momenta, because this ratio goes to zero for high values of P .

Chapter 3

Momentum distributions in the ReCo formalism

3.1 Introduction to the formalism

In this chapter, we describe mathematically the process of coalescence (or recombination, ReCo for short), in a way that does not have the limitations of the simple model that was discussed in the previous chapter. We use a relatively sophisticated method, that combines the quantum mechanical density operator with a relativistic space-time description. In the past, this method has also been employed to describe the coalescence of hadrons into small nuclei after heavy ion collisions [8]. Of course, we will be interested in the earlier stage after such a collision, in which partons coalesce to form hadrons.

One of the shortcomings of the model that was treated in the previous chapter was that it was a static description of what happens inside a constant volume, whereas in reality one would expect the volume to expand rapidly immediately after the heavy ion collision has taken place. Therefore, in a more sophisticated description we should include this expansion, using the concept of particle flow: the number of particles that crosses a unit surface element of a cylindrical surface.

Furthermore, a homogeneous description of the recombining partons cannot be a generally valid one. We must allow for a more general parton density. We shall use matrix elements of the quantum mechanical density operator, which will subsequently be incorporated into the definition of a so-called two-particle Wigner function. The role of this Wigner function in the equations for the hadron momentum distribution will be similar to the role previously played by the product of parton phase space distributions.

It will quickly become clear that there is a price that we have to pay for the increased realism of our description of the recombination process. The simplicity and (relative) transparency of the previous model are dropped in favor of more complicated-looking expressions and

concepts. Later on however, we will want to make our results more concrete to be able to make the connection with experiment. In order to achieve this, we will make assumptions and simplifications which effectively bring us a bit closer again to the (more limited) model of the previous chapter.

As in the previous chapter, the derivations are presented in an extensive step-by-step manner for mesons, followed by a more concise treatment of baryons. The main object in this chapter will be to find expressions for the momentum distribution of mesons and baryons that originate from coalescing partons. In the next chapter, we will use those expressions to calculate the quantity that is known as “elliptic flow”, both for partons and for hadrons.

3.2 The quantum mechanical density operator

Starting point of our derivations concerning the meson momentum distribution, is the following equation, which relates the quantum mechanical density operator $\hat{\rho}_{ab}$ to the total number of mesons of type M [3, 8]:

$$N_M = \sum_{a,b} \int \frac{d^3P}{(2\pi)^3} \langle M \mathbf{P} | \hat{\rho}_{ab} | M \mathbf{P} \rangle. \quad (3.2.1)$$

This formula can be understood in the following way. The quantum mechanical expectation value of the physical quantity associated with the operator $\hat{\rho}_{ab}$ for a meson M in state $| M \mathbf{P} \rangle$ is

$$\langle M \mathbf{P} | \hat{\rho}_{ab} | M \mathbf{P} \rangle. \quad (3.2.2)$$

The indices a and b denote the quantum numbers of the two quark states that make up this meson state. The physical interpretation of $\hat{\rho}_{ab}$ is then such that we interpret

$$\frac{d^3P}{(2\pi)^3} \langle M \mathbf{P} | \hat{\rho}_{ab} | M \mathbf{P} \rangle \quad (3.2.3)$$

as the expected number of mesons of type M (consisting of quarks with quantum numbers a and b) that have their momenta in a three-dimensional momentum interval d^3P around \mathbf{P} . Now equation (3.2.1) follows naturally, because the total number of mesons of type M consists of mesons M of all momenta and of all possible combinations of quarks that make up this particular meson.

Inserting two completeness relations into the right side of (3.2.1), we may write the total number of mesons M as

$$N_M = \sum_{a,b} \int \frac{d^3P}{(2\pi)^3} d^3\hat{r}_1 d^3\hat{r}'_1 d^3\hat{r}_2 d^3\hat{r}'_2 \langle M \mathbf{P} | \hat{\mathbf{r}}_1, \hat{\mathbf{r}}_2 \rangle \langle \hat{\mathbf{r}}_1, \hat{\mathbf{r}}_2 | \hat{\rho}_{ab} | \hat{\mathbf{r}}'_1, \hat{\mathbf{r}}'_2 \rangle \langle \hat{\mathbf{r}}'_1, \hat{\mathbf{r}}'_2 | M \mathbf{P} \rangle. \quad (3.2.4)$$

Next we perform a change of variables to $\mathbf{r}_{1,2} = (\hat{\mathbf{r}}_{1,2} + \hat{\mathbf{r}}'_{1,2})/2$ and $\mathbf{r}'_{1,2} = \hat{\mathbf{r}}_{1,2} - \hat{\mathbf{r}}'_{1,2}$. This leads to

$$N_M = \sum_{a,b} \int \frac{d^3 P}{(2\pi)^3} d^3 r_1 d^3 r'_1 d^3 r_2 d^3 r'_2 \langle M \mathbf{P} | \mathbf{r}_1 + \frac{\mathbf{r}'_1}{2}, \mathbf{r}_2 + \frac{\mathbf{r}'_2}{2} \rangle \\ \times \langle \mathbf{r}_1 + \frac{\mathbf{r}'_1}{2}, \mathbf{r}_2 + \frac{\mathbf{r}'_2}{2} | \hat{\rho}_{ab} | \mathbf{r}_1 - \frac{\mathbf{r}'_1}{2}, \mathbf{r}_2 - \frac{\mathbf{r}'_2}{2} \rangle \langle \mathbf{r}_1 - \frac{\mathbf{r}'_1}{2}, \mathbf{r}_2 - \frac{\mathbf{r}'_2}{2} | M \mathbf{P} \rangle. \quad (3.2.5)$$

It should be noted, however, that the use of these time-independent completeness relations is associated with an equal-time approach.

3.3 Wigner functions

At this point we introduce the two-particle Wigner function $W_{ab}(\mathbf{r}_1, \mathbf{r}_2; \mathbf{p}_1, \mathbf{p}_2)$. It is defined to be such that

$$\langle \mathbf{r}_1 + \frac{\mathbf{r}'_1}{2}, \mathbf{r}_2 + \frac{\mathbf{r}'_2}{2} | \hat{\rho}_{ab} | \mathbf{r}_1 - \frac{\mathbf{r}'_1}{2}, \mathbf{r}_2 - \frac{\mathbf{r}'_2}{2} \rangle = \int \frac{d^3 p_1}{(2\pi)^3} \frac{d^3 p_2}{(2\pi)^3} e^{-i\mathbf{p}_1 \cdot \mathbf{r}'_1} e^{-i\mathbf{p}_2 \cdot \mathbf{r}'_2} W_{ab}(\mathbf{r}_1, \mathbf{r}_2; \mathbf{p}_1, \mathbf{p}_2). \quad (3.3.1)$$

Furthermore, we define the internal meson wave function φ_M through

$$\langle \mathbf{r}_1 + \frac{\mathbf{r}'_1}{2}, \mathbf{r}_2 + \frac{\mathbf{r}'_2}{2} | M \mathbf{P} \rangle = e^{-i\mathbf{P} \cdot (\mathbf{R} + \mathbf{R}'/2)} \varphi_M \left(\mathbf{r} - \frac{\mathbf{r}'}{2} \right), \quad (3.3.2)$$

where \mathbf{R} , \mathbf{r} , \mathbf{R}' and \mathbf{r}' are the usual centre-of-mass and relative coordinates:

$$\mathbf{R}^{(\prime)} = (\mathbf{r}_1^{(\prime)} + \mathbf{r}_2^{(\prime)})/2; \\ \mathbf{r}^{(\prime)} = \mathbf{r}_1^{(\prime)} - \mathbf{r}_2^{(\prime)}. \quad (3.3.3)$$

For the momenta, we define

$$\tilde{\mathbf{P}} = \mathbf{p}_1 + \mathbf{p}_2; \\ \mathbf{q} = (\mathbf{p}_1 - \mathbf{p}_2)/2. \quad (3.3.4)$$

With these definitions, (3.2.5) becomes

$$\begin{aligned}
N_M &= \sum_{ab} \int \frac{d^3 P}{(2\pi)^3} \frac{d^3 p_1}{(2\pi)^3} \frac{d^3 p_2}{(2\pi)^3} d^3 r_1 d^3 r'_1 d^3 r_2 d^3 r'_2 \times \\
&\times e^{+i\mathbf{P}\cdot(\mathbf{R}+\mathbf{R}'/2)} \varphi_M^* \left(\mathbf{r} - \frac{\mathbf{r}'}{2} \right) e^{-i\mathbf{p}_1\cdot\mathbf{r}'_1} e^{-i\mathbf{p}_2\cdot\mathbf{r}'_2} W_{ab}(\mathbf{r}_1, \mathbf{r}_2; \mathbf{p}_1, \mathbf{p}_2) e^{-i\mathbf{P}\cdot(\mathbf{R}-\mathbf{R}'/2)} \varphi_M \left(\mathbf{r} + \frac{\mathbf{r}'}{2} \right) \\
&= \sum_{ab} \int \frac{d^3 P}{(2\pi)^3} \frac{d^3 \tilde{P}}{(2\pi)^3} \frac{d^3 q}{(2\pi)^3} d^3 R d^3 R' d^3 r d^3 r' e^{i\mathbf{P}\cdot\mathbf{R}'} \varphi_M^* \left(\mathbf{r} - \frac{\mathbf{r}'}{2} \right) \times \\
&\quad \times e^{-i\tilde{\mathbf{P}}\cdot\mathbf{R}' - i\mathbf{q}\cdot\mathbf{r}'} W_{ab} \left(\mathbf{R} + \frac{\mathbf{r}}{2}, \mathbf{R} - \frac{\mathbf{r}}{2}; \frac{\tilde{\mathbf{P}}}{2} + \mathbf{q}, \frac{\tilde{\mathbf{P}}}{2} - \mathbf{q} \right) \varphi_M \left(\mathbf{r} + \frac{\mathbf{r}'}{2} \right) \\
&= \sum_{ab} \int \frac{d^3 P}{(2\pi)^3} \frac{d^3 \tilde{P}}{(2\pi)^3} \frac{d^3 q}{(2\pi)^3} d^3 R d^3 r d^3 r' \left(\int d^3 R' e^{i(\mathbf{P}-\tilde{\mathbf{P}})\cdot\mathbf{R}'} \right) \times \\
&\quad \times W_{ab} \left(\mathbf{R} + \frac{\mathbf{r}}{2}, \mathbf{R} - \frac{\mathbf{r}}{2}; \frac{\tilde{\mathbf{P}}}{2} + \mathbf{q}, \frac{\tilde{\mathbf{P}}}{2} - \mathbf{q} \right) e^{-i\mathbf{q}\cdot\mathbf{r}'} \varphi_M \left(\mathbf{r} + \frac{\mathbf{r}'}{2} \right) \varphi_M^* \left(\mathbf{r} - \frac{\mathbf{r}'}{2} \right). \quad (3.3.5)
\end{aligned}$$

We can evaluate the integral over \mathbf{R}' , which yields a delta function: $\int d^3 R' e^{i(\mathbf{P}-\tilde{\mathbf{P}})\cdot\mathbf{R}'} = (2\pi)^3 \delta^{(3)}(\mathbf{P} - \tilde{\mathbf{P}})$. Then we can integrate out this delta function, and we are left with

$$\begin{aligned}
N_M &= \sum_{a,b} \int \frac{d^3 P}{(2\pi)^3} \frac{d^3 q}{(2\pi)^3} \int d^3 R d^3 r W_{ab} \left(\mathbf{R} + \frac{\mathbf{r}}{2}, \mathbf{R} - \frac{\mathbf{r}}{2}; \frac{\mathbf{P}}{2} + \mathbf{q}, \frac{\mathbf{P}}{2} - \mathbf{q} \right) \times \\
&\quad \times \int d^3 r' e^{-i\mathbf{q}\cdot\mathbf{r}'} \varphi_M \left(\mathbf{r} + \frac{\mathbf{r}'}{2} \right) \varphi_M^* \left(\mathbf{r} - \frac{\mathbf{r}'}{2} \right). \quad (3.3.6)
\end{aligned}$$

Let's define the function

$$\Phi_M^W(\mathbf{r}, \mathbf{q}) = \int d^3 r' e^{-i\mathbf{q}\cdot\mathbf{r}'} \varphi_M \left(\mathbf{r} + \frac{\mathbf{r}'}{2} \right) \varphi_M^* \left(\mathbf{r} - \frac{\mathbf{r}'}{2} \right). \quad (3.3.7)$$

This function can actually be interpreted as the Wigner function of the meson of type M . With this definition, we can immediately turn (3.3.6) into the following formula for the momentum distribution of mesons of type M :

$$\frac{dN_M}{d^3 P} = (2\pi)^{-3} \sum_{a,b} \int d^3 R \int \frac{d^3 q}{(2\pi)^3} \frac{d^3 r}{(2\pi)^3} W_{ab} \left(\mathbf{R} + \frac{\mathbf{r}}{2}, \mathbf{R} - \frac{\mathbf{r}}{2}; \frac{\mathbf{P}}{2} + \mathbf{q}, \frac{\mathbf{P}}{2} - \mathbf{q} \right) \Phi_M^W(\mathbf{r}, \mathbf{q}). \quad (3.3.8)$$

3.4 Lorentz invariance

At this point, it is necessary to get our notation completely clear. From here onward, four-vectors will be denoted by (for example) p or p^μ , and inner products of four-vectors by $p \cdot k$

or explicitly by $p^\mu k_\mu$. The metric tensor we will use is $g = \text{diag}(1, -1, -1, -1)$. By p^2 we will mean the inner product of the *four*-vector p and itself. On the other hand, three-vectors we will keep on denoting by boldface symbols. In measures, like d^3P , we will not use boldface symbols for three-vectors, since the dimension is clear from the superscript on the d .

We replace the measure $d^3P d^3R$ by

$$d^3P d^3R P \cdot u(R)/E, \quad (3.4.1)$$

which is manifestly Lorentz invariant at fixed R ($P \cdot u(R)$ is an inner product of four-vectors and d^3P/E is also Lorentz invariant, which can be derived from the fact that $d^4P \delta(P^2 - M^2)$ is Lorentz invariant). Here, the unit vector $u(R)$ is future oriented. Future is defined as the direction that is orthogonal to the hypersurface Σ (over which we integrate) which in turn is defined by the hadronization volume. We check that in the case of $u = (1, 0, 0, 0)$ (which defines a hypersurface of constant time), we simply have $P \cdot u/E = E/E = 1$. Though instead of the choice $t = \text{constant}$, we will be interested in the hadronization hypersurface described by the constraint that $\tau = \sqrt{t^2 - z^2}$ is constant (see section 3.9).

3.5 Simplifications

There is a number of simplifications that can be made in expression (3.3.8). First, we assume that the two-particle Wigner function W_{ab} can be factorized into two (classical) one-particle phase space distributions w_a and w_b . This can be interpreted to mean that the phase space distributions of the two coalescing partons are independent of each other *before* the recombination process takes place [1]. Secondly, we replace the summation over the quantum numbers a and b by a degeneracy factor C_M . The assumption behind this action is, that the parton phase space distribution is the same for each flavor. This means we can drop all a 's and b 's. Summarizing these changes, we write

$$\sum_{ab} W_{ab} \left(\mathbf{R} + \frac{\mathbf{r}}{2}, \mathbf{R} - \frac{\mathbf{r}}{2}; \frac{\mathbf{P}}{2} + \mathbf{q}, \frac{\mathbf{P}}{2} - \mathbf{q} \right) \rightarrow C_M w \left(\mathbf{R} + \frac{\mathbf{r}}{2}; \frac{\mathbf{P}}{2} + \mathbf{q} \right) w \left(\mathbf{R} - \frac{\mathbf{r}}{2}; \frac{\mathbf{P}}{2} - \mathbf{q} \right). \quad (3.5.1)$$

But there is more that we can do to simplify our meson momentum distribution. Let us take a good look at the integrand of (3.3.8), but with the Wigner function W_{ab} factorized as described above. The spatial width of the meson Wigner function Φ_M^W (which we will denote by Δr) is determined by the width of the hadron wave function φ_M . Since the width of this hadron wave function (the typical size of a hadron) can be assumed to be small when compared to the size of the total system at hadronization (which should be roughly the size of a nucleus), we can say that the spatial width of Φ_M^W , too, will be small when compared to the size of the system at hadronization. So for both factors of the parton phase space distribution, only the region where $\|\mathbf{r}\| \approx \Delta r$, actually contributes to the outcome of the integral. We can assume that the parton phase space distribution does not vary much in this

small region of \mathbf{r} , and consequently we may omit the \mathbf{r} -dependence in both factors of w . The effect of this reasoning can be written as

$$w\left(\mathbf{R} + \frac{\mathbf{r}}{2}; \frac{\mathbf{P}}{2} + \mathbf{q}\right) w\left(\mathbf{R} - \frac{\mathbf{r}}{2}; \frac{\mathbf{P}}{2} - \mathbf{q}\right) \rightarrow w\left(R; \frac{\mathbf{P}}{2} + \mathbf{q}\right) w\left(R; \frac{\mathbf{P}}{2} - \mathbf{q}\right). \quad (3.5.2)$$

With these two changes, our meson momentum distribution reduces to

$$E \frac{dN_M}{d^3P} = C_M \int_{\Sigma} \frac{d^3R P \cdot u(R)}{(2\pi)^3} \int \frac{d^3q d^3r}{(2\pi)^3} w\left(R; \frac{\mathbf{P}}{2} - \mathbf{q}\right) \Phi_M^W(\mathbf{r}, \mathbf{q}) w\left(R; \frac{\mathbf{P}}{2} + \mathbf{q}\right). \quad (3.5.3)$$

Since now the only remaining \mathbf{r} -dependence is in $\Phi_M^W(\mathbf{r}, \mathbf{q})$, it is natural to define

$$\Phi_M^W(\mathbf{q}) = \int d^3r \Phi_M^W(\mathbf{r}, \mathbf{q}), \quad (3.5.4)$$

and we are left with the expression

$$E \frac{dN_M}{d^3P} = C_M \int_{\Sigma} \frac{d^3R P \cdot u(R)}{(2\pi)^3} \int \frac{d^3q}{(2\pi)^3} w\left(R; \frac{\mathbf{P}}{2} - \mathbf{q}\right) \Phi_M^W(\mathbf{q}) w\left(R; \frac{\mathbf{P}}{2} + \mathbf{q}\right). \quad (3.5.5)$$

3.6 Using light cone coordinates

We let the hadron momentum \mathbf{P} define the z -axis of the so-called hadron light cone (HLC) frame. Vector components that are orthogonal to this direction will be denoted by the subscript “ \perp ”, so that we can use “ T ” as a subscript for vectors that are orthogonal to the beam axis. We define light cone coordinates in the usual way, i.e.

$$p^+ = \frac{p^0 + p^z}{\sqrt{2}}; \quad (3.6.1)$$

$$p^- = \frac{p^0 - p^z}{\sqrt{2}}. \quad (3.6.2)$$

So for the hadron we have $P^+ = (E + \|\mathbf{P}\|)/\sqrt{2}$, since \mathbf{P} is in the z -direction in the HLC frame.

We want to change variables in the momentum integral (3.5.5) to light-cone coordinates. This means we have to replace our integration over the relative three-momentum \mathbf{q} by an appropriate integration over light-cone coordinates. To find out what this should look like, we first reintroduce the three-momentum of one of the two partons in the meson,

$$\mathbf{k} = \mathbf{P}/2 - \mathbf{q}. \quad (3.6.3)$$

Next, we note that, for any function $F(\mathbf{k})$,

$$\int d^4k 2k^0 \delta(k^2 - m^2) F(\mathbf{k}) = \int d^3k dk^0 2k^0 \delta(k^{02} - (\mathbf{k}^2 + m^2)) F(\mathbf{k}). \quad (3.6.4)$$

We can use the well-known identity $\delta(f(x)) = \sum_i \frac{\delta(x-x_i)}{|f'(x_i)|}$ (where the x_i are the zeros of f), to work this out to

$$\int d^3k dk^0 2k^0 \left(\frac{\delta(k^0 + \sqrt{\mathbf{k}^2 + m^2})}{2\sqrt{\mathbf{k}^2 + m^2}} + \frac{\delta(k^0 - \sqrt{\mathbf{k}^2 + m^2})}{2\sqrt{\mathbf{k}^2 + m^2}} \right) F(\mathbf{k}). \quad (3.6.5)$$

But since we only integrate over positive values of k^0 (we do not take further parton interactions into account), the first term will not contribute. Integrating out the remaining delta function, we may conclude that

$$\int d^4k 2k^0 \delta(k^2 - m^2) F(\mathbf{k}) = \int d^3k F(\mathbf{k}). \quad (3.6.6)$$

On the other hand, using light-cone momenta, we can write

$$\begin{aligned} \int d^4k 2k^0 \delta(k^2 - m^2) F(\mathbf{k}) &= \int dk^+ d^2k^\perp dk^- 2 \frac{(k^+ + k^-)}{\sqrt{2}} \delta(2k^+k^- - \mathbf{k}^{\perp 2} - m^2) F(\mathbf{k}) \\ &= \int dk^+ d^2k^\perp dk^- \sqrt{2}(k^+ + k^-) \frac{\delta(k^- - \frac{(\mathbf{k}^{\perp 2} + m^2)}{2k^+})}{2k^+} F(\mathbf{k}) \\ &= \int dk^+ d^2k^\perp \frac{1}{\sqrt{2}} \frac{(k^+ + \frac{(\mathbf{k}^{\perp 2} + m^2)}{2k^+})}{k^+} F(\mathbf{k}) = \int dk^+ d^2k^\perp \frac{1}{\sqrt{2}} \left(1 + \frac{(\mathbf{k}^{\perp 2} + m^2)}{2k^{+2}} \right) F(\mathbf{k}) \\ &\simeq \int dk^+ d^2k^\perp \frac{1}{\sqrt{2}} F(\mathbf{k}), \end{aligned} \quad (3.6.7)$$

where the last step is only justified if the function $F(\mathbf{k})$ is sufficiently small when k^+ is small, which it is indeed in our case (cf. expression (3.5.5)).

Combining equations (3.6.6) and (3.6.7), we find

$$\int d^3k F(\mathbf{k}) = \int dk^+ d^2k^\perp \frac{1}{\sqrt{2}} F(\mathbf{k}). \quad (3.6.8)$$

This identity effectively enables us to replace the measure d^3k in our integral (3.5.5) by $dk^+ d^2k^\perp/\sqrt{2}$. Furthermore, we define a new parameter, x , as the ratio of light-cone parton momentum and light-cone hadron momentum:

$$k^+ = xP^+. \quad (3.6.9)$$

The resulting expression, in light-cone coordinates, for the spectrum of mesons of type M is

$$E \frac{dN_M}{d^3P} = C_M \int_\Sigma \frac{d^3R P \cdot u(R)}{(2\pi)^3} \int \frac{dx P^+ d^2k_\perp}{\sqrt{2}(2\pi)^3} w(R; xP^+, \mathbf{k}_\perp) \Phi_M^W(x, \mathbf{k}_\perp) w(R; (1-x)P^+, -\mathbf{k}_\perp). \quad (3.6.10)$$

In the argument of the second parton distribution factor, we have $(1-x)P^+$ and $-\mathbf{k}_\perp$ because $\mathbf{P}/2 + \mathbf{q} = \mathbf{P} - \mathbf{k}$, so in light cone coordinates the $+$ component becomes $P^+ - xP^+ = (1-x)P^+$, and the transverse components (transverse to \mathbf{P} , not to the beam axis) become $\mathbf{0} - \mathbf{k}_\perp = -\mathbf{k}_\perp$.

3.7 Factorized meson Wigner function

Let us have a closer look at the spatially integrated Wigner function $\Phi_M^W(\mathbf{q})$. From the definition of $\Phi_M^W(\mathbf{r}, \mathbf{q})$ it is easily seen that $\Phi_M^W(\mathbf{q})$ is in fact a real function, since it equals its complex conjugate. Moreover, (because of its physical interpretation) it must be a non-negative function. This means we can write it as the absolute value squared of another function:

$$\Phi_M^W(x, \mathbf{k}_\perp) = |\bar{\phi}_M(x, \mathbf{k}_\perp)|^2. \quad (3.7.1)$$

Next, we make the following factorized *Ansatz*:

$$\bar{\phi}_M(x, \mathbf{k}_\perp) = \phi_M(x)\Omega(k_\perp). \quad (3.7.2)$$

We expect that the coalescing partons have their momenta almost entirely in the direction of the resulting hadron. Therefore, we expect that the width of Ω , which we will call Λ_\perp , is small compared to P^+ . Furthermore, we assume that the variation of the parton distribution w is small with respect to variations of \mathbf{k}_\perp within the small width Λ_\perp . Then it is justified for us to omit the \mathbf{k}_\perp -dependence in both factors of w . Consequently, the only remaining \mathbf{k}_\perp -dependence is in the function $\Omega(k_\perp)$, and we can integrate this out using the normalization

$$\int \frac{dx P^+ d^2 k_\perp}{\sqrt{2}(2\pi)^3} \Phi_M^W(x, \mathbf{k}_\perp) = 1, \quad (3.7.3)$$

leading to the result

$$E \frac{dN_M}{d^3 P} = C_M \int_\Sigma \frac{d^3 R P \cdot u(R)}{(2\pi)^3} \int_0^1 dx w(R; xP^+) |\phi_M(x)|^2 w(R; (1-x)P^+). \quad (3.7.4)$$

Remember we defined the parameter x as the ratio of light-cone parton momentum and light-cone hadron momentum:

$$k^+ = xP^+. \quad (3.7.5)$$

We want to know what this means for the relation between x and the *normal* parton and hadron momenta \mathbf{k} and \mathbf{P} . To find out, we plug in the definitions of k^+ and P^+ . Then equation (3.7.5) reads

$$k^0 + k^3 = x(E + \|\mathbf{P}\|). \quad (3.7.6)$$

We can approximate the hadron energy E by using a Taylor expansion for large hadron momentum $\|\mathbf{P}\|$:

$$E = \sqrt{\|\mathbf{P}\|^2 + M^2} = \|\mathbf{P}\| \sqrt{1 + \frac{M^2}{\|\mathbf{P}\|^2}} \simeq \|\mathbf{P}\| + \frac{1}{2} \frac{M^2}{\|\mathbf{P}\|}. \quad (3.7.7)$$

Assuming also a large *parton* momentum, we may similarly approximate

$$k^0 = \sqrt{\|\mathbf{k}\|^2 + m^2} \simeq \|\mathbf{k}\| + \frac{1}{2} \frac{m^2}{\|\mathbf{k}\|}. \quad (3.7.8)$$

With these approximations, equation (3.7.6) becomes

$$\|\mathbf{k}\| + \frac{1}{2} \frac{m^2}{\|\mathbf{k}\|} + k^3 = x \left(\|\mathbf{P}\| + \frac{1}{2} \frac{M^2}{\|\mathbf{P}\|} + \|\mathbf{P}\| \right), \quad (3.7.9)$$

or

$$\|\mathbf{k}\| + k^3 = 2x\|\mathbf{P}\| + \mathcal{O} \left(x \frac{M^2}{\|\mathbf{P}\|} \right) + \mathcal{O} \left(\frac{m^2}{\|\mathbf{k}\|} \right). \quad (3.7.10)$$

Since Λ_\perp , the width of $\Omega(\mathbf{k}_\perp)$, is small (as was explained earlier in this section), we can replace k^3 by

$$\|\mathbf{k}\| + \mathcal{O}(\Lambda_\perp), \quad (3.7.11)$$

and we arrive at¹

$$\mathbf{k} = x\mathbf{P} + \mathcal{O} \left(x \frac{M^2}{\|\mathbf{P}\|} \right) + \mathcal{O} \left(\frac{m^2}{\|\mathbf{k}\|} \right) + \mathcal{O}(\Lambda_\perp), \quad (3.7.12)$$

so x can also be interpreted as the “normal” momentum fraction of one of the two quarks that coalesce into the meson of type M . We can replace P^+ with \mathbf{P} in the momentum distribution integral (3.7.4) since we are looking at high hadron momenta. So for mesons of type M we have

$$E \frac{dN_M}{d^3P} = C_M \int_\Sigma \frac{d\sigma_R P \cdot u(R)}{(2\pi)^3} \int_0^1 dx w(R; x\mathbf{P}) |\phi_M(x)|^2 w(R; (1-x)\mathbf{P}), \quad (3.7.13)$$

and for baryons of type B , the resulting expression is

$$E \frac{dN_B}{d^3P} = C_B \int_\Sigma \frac{d\sigma_R P \cdot u(R)}{(2\pi)^3} \int \mathcal{D}x w(R; x_1\mathbf{P}) w(R; x_2\mathbf{P}) w(R; x_3\mathbf{P}) |\phi_B(x_1, x_2, x_3)|^2, \quad (3.7.14)$$

where the measure $\int \mathcal{D}x$ stands for $\int_0^1 \int_0^1 \int_0^1 dx_1 dx_2 dx_3 \delta(x_1 + x_2 + x_3 - 1)$.

3.8 Results for narrow longitudinal functions

To get further insight into the results of our calculations, in this section we make the approximation that the longitudinal distribution amplitudes $\phi_M(x)$ and $\phi_B(x_1, x_2, x_3)$ are very narrow and centered around the expected momentum fractions. Obviously, the limiting cases for narrow functions are delta functions. For mesons, the natural choice is to assign a momentum fraction of $1/2$ to each parton. Of course, for baryons we choose the value $1/3$. Thus we arrive at the following delta function approximations:

$$|\phi_M(x)|^2 = \delta \left(x - \frac{1}{2} \right), \quad (3.8.1)$$

$$|\phi_B(x_1, x_2, x_3)|^2 = \delta \left(x_1 - \frac{1}{3} \right) \delta \left(x_2 - \frac{1}{3} \right). \quad (3.8.2)$$

¹In Ref. [3], the $\mathcal{O} \left(\frac{m^2}{\|\mathbf{k}\|} \right)$ -term is absent.

These lead to the expressions

$$E \frac{dN_M}{d^3P} = C_M \int_{\Sigma} \frac{d\sigma_R P \cdot u(R)}{(2\pi)^3} w\left(R; \frac{\mathbf{P}}{2}\right) w\left(R; \frac{\mathbf{P}}{2}\right) \quad (3.8.3)$$

and

$$E \frac{dN_B}{d^3P} = C_B \int_{\Sigma} \frac{d\sigma_R P \cdot u(R)}{(2\pi)^3} w\left(R; \frac{\mathbf{P}}{3}\right) w\left(R; \frac{\mathbf{P}}{3}\right) w\left(R; \frac{\mathbf{P}}{3}\right). \quad (3.8.4)$$

3.9 The hadronization hypersurface

In order to be able to work out the integral in equations (3.7.13) and (3.7.14), we need a parametrization of the hadronization hypersurface Σ . We parametrize Σ as follows:

$$R^\mu = (t, x, y, z) = (\tau \cosh \eta, \rho \cos \phi, \rho \sin \phi, \tau \sinh \eta), \quad (3.9.1)$$

where our parameters ρ and ϕ are the usual cylindrical coordinates, and the parameter η is called the “space-time rapidity”, which is defined by $\eta = \frac{1}{2} \log \left(\frac{t+z}{t-z} \right)$. This definition is analogous to the definition of the familiar rapidity variable $y = \frac{1}{2} \log \left(\frac{p^0+p^z}{p^0-p^z} \right)$.

We choose to look at hypersurfaces of constant proper time $\tau = \sqrt{t^2 - z^2}$. The motivation for this condition lies in the fact that we expect all particle distributions to be approximately independent of the space-time rapidity η [10, 11]. If we introduce $t^+ = t + z$ and $t^- = t - z$, we can write $\tau = \sqrt{t^2 - z^2}$ as $\tau = t^+ t^-$. A longitudinal Lorentz boost would transform

$$t^+ \rightarrow t^{+'} = t' + z' = \frac{1 - \beta}{\sqrt{1 - \beta^2}}(t + z) = \sqrt{\frac{1 - \beta}{1 + \beta}} t^+ = e^\eta t^+, \quad (3.9.2)$$

and

$$t^- \rightarrow t^{-'} = t' - z' = \frac{1 + \beta}{\sqrt{1 - \beta^2}}(t - z) = \sqrt{\frac{1 + \beta}{1 - \beta}} t^- = e^{-\eta} t^-. \quad (3.9.3)$$

It follows that $\tau = t^+ t^-$ is invariant under longitudinal Lorentz boosts. Therefore distributions are the same on hypersurfaces of constant τ .

Of course, we want to know what form the measure $d\sigma_R$ takes under the chosen parametrization. This can be calculated straightforwardly from the chosen parametrization by taking the square root of the determinant of the pullback metric tensor:

$$d\sigma_R = \sqrt{-\det \bar{g}} d\eta d\rho d\phi, \quad (3.9.4)$$

where the 3×3 pullback tensor \bar{g} is defined as

$$\bar{g}_{rs} = \frac{\partial R^\mu}{\partial \sigma^r} \frac{\partial R^\nu}{\partial \sigma^s} g_{\mu\nu}, \quad (3.9.5)$$

with $r, s \in \{0, 1, 2\}$. Remember that we chose the metric tensor $g = \text{diag}(1, -1, -1, -1)$. We explicitly calculate the components of the pullback tensor, choosing $\sigma^0 = \eta$, $\sigma^1 = \rho$, and $\sigma^2 = \phi$:

$$\begin{aligned}
\bar{g}_{00} &= \frac{\partial R^\mu}{\partial \eta} \frac{\partial R^\nu}{\partial \eta} g_{\mu\nu} = \frac{\partial R^0}{\partial \eta} \frac{\partial R^0}{\partial \eta} - 0 - 0 - \frac{\partial R^3}{\partial \eta} \frac{\partial R^3}{\partial \eta} = \tau^2 \sinh^2 \eta - \tau^2 \cosh^2 \eta = -\tau^2; \\
\bar{g}_{11} &= -\frac{\partial R^1}{\partial \rho} \frac{\partial R^1}{\partial \rho} - \frac{\partial R^2}{\partial \rho} \frac{\partial R^2}{\partial \rho} = -\cos^2 \phi - \sin^2 \phi = -1; \\
\bar{g}_{22} &= -\frac{\partial R^1}{\partial \phi} \frac{\partial R^1}{\partial \phi} - \frac{\partial R^2}{\partial \phi} \frac{\partial R^2}{\partial \phi} = -\rho^2 \sin^2 \phi - \rho^2 \cos^2 \phi = -\rho^2; \\
\bar{g}_{01} &= \bar{\eta}_{10} = 0; \\
\bar{g}_{02} &= \bar{\eta}_{20} = 0; \\
\bar{g}_{12} &= \bar{\eta}_{21} = -\frac{\partial R^1}{\partial \rho} \frac{\partial R^1}{\partial \phi} - \frac{\partial R^2}{\partial \rho} \frac{\partial R^2}{\partial \phi} = \rho \cos \phi \sin \phi - \rho \sin \phi \cos \phi = 0.
\end{aligned} \tag{3.9.6}$$

From this we conclude

$$d\sigma_R = \sqrt{-\begin{vmatrix} -\tau^2 & 0 & 0 \\ 0 & -1 & 0 \\ 0 & 0 & -\rho^2 \end{vmatrix}} d\eta d\rho d\phi = \sqrt{\tau^2 \rho^2} d\eta d\rho d\phi = \tau \rho d\eta d\rho d\phi. \tag{3.9.7}$$

The unit vector normal to the hypersurface that we have defined, is parametrized by

$$u^\mu = (\cosh \eta, 0, 0, \sinh \eta). \tag{3.9.8}$$

To verify that this vector is indeed normal to the hadronization hypersurface, we show that it is normal to all three tangent vectors to this surface:

$$\begin{aligned}
\frac{\partial R^\mu}{\partial \eta} u_\mu &= (\tau \sinh \eta \quad 0 \quad 0 \quad \tau \cosh \eta) \begin{pmatrix} \cosh \eta \\ 0 \\ 0 \\ -\sinh \eta \end{pmatrix} \\
&= \tau \sinh \eta \cosh \eta - \tau \cosh \eta \sinh \eta = 0;
\end{aligned} \tag{3.9.9}$$

$$\frac{\partial R^\mu}{\partial \rho} u_\mu = (0 \quad \cos \phi \quad \sin \phi \quad 0) \begin{pmatrix} \cosh \eta \\ 0 \\ 0 \\ -\sinh \eta \end{pmatrix} = 0; \tag{3.9.10}$$

$$\frac{\partial R^\mu}{\partial \phi} u_\mu = (0 \quad -\rho \sin \phi \quad \rho \cos \phi \quad 0) \begin{pmatrix} \cosh \eta \\ 0 \\ 0 \\ -\sinh \eta \end{pmatrix} = 0. \tag{3.9.11}$$

For future convenience, it is useful to calculate the inner product $p^\mu u_\mu$ of the parton four-momentum and the four-vector normal to the hadronization surface. The parton momentum four-vector can be parametrized, using the so-called transverse mass $m_T = \sqrt{m^2 + p_T^2}$, as

$$p^\mu = (m_T \cosh y, p_T \cos \Phi, p_T \sin \Phi, m_T \sinh y). \quad (3.9.12)$$

Here, $y = \frac{1}{2} \log \left(\frac{p^0 + p^3}{p^0 - p^3} \right)$ is the usual rapidity variable, which is indeed such that $p^0 = \sqrt{p^{02} - p^{32}} \cosh y = m_T \cosh y$ and $p^3 = m_T \sinh y$. Now it is straightforward to calculate that

$$\begin{aligned} p \cdot u &= p^\mu u_\mu = p^0 u^0 - \mathbf{p} \cdot \mathbf{u} = m_T \cosh y \cosh \eta - m_T \sinh y \sinh \eta \\ &= m_T \cosh(\eta - y). \end{aligned} \quad (3.9.13)$$

3.10 The parton phase

To make our calculations more concrete, we should also take a closer look at the parton phase immediately after the heavy ion collision. At low and intermediate values of the transverse parton momentum p_T , we expect dominance of thermalized partons with a certain temperature T that recombine into hadrons. In other words, we expect an exponential spectrum. Therefore, we write the parton phase space distribution as²

$$w(R; p) = \gamma e^{-p \cdot v(R)/T} e^{-\eta^2/2\Delta^2} f(\rho, \phi). \quad (3.10.1)$$

In this formula, the chemical potential-dependent factor $\gamma = e^{\mu/T}$ is called fugacity. The product $e^{-\eta^2/2\Delta^2} f(\rho, \phi)$ describes the space-time structure of the parton source. The first factor is a broad Gaussian centered around zero space-time rapidity, the second factor describes the transverse shape of the source. We assume that the transverse distribution f is homogeneous (equal to 1) as long as the radial coordinate ρ is smaller than a certain radius ρ_0 , and that it equals zero otherwise. One might say we view the source as a homogeneous disc in the transverse plane, with radius ρ_0 . We make use of the Heaviside function Θ and write it as

$$f(\rho, \phi) = \Theta(\rho_0 - \rho). \quad (3.10.2)$$

This will make it very easy to perform future ρ and ϕ integrals. Of course, the omission of a ϕ -dependence of f can only be right in the case of *central* heavy ion collisions (zero impact parameter). That is what we will be studying here; the alternative case, non-centrality, will be treated extensively in the next chapter.

We want to know whether perhaps we can assume the Gaussian $e^{-\eta^2/2\Delta^2}$ to be so broad that we can approximate it by the constant function 1. This will only be possible if the $\eta^2/2\Delta^2$

²Note that we do not include a normalization factor in the formula for $w(R; p)$. As a result, all momentum distributions that we will derive from this parton phase space distribution are correct up to a normalization factor.

in the exponent is small when compared to $p \cdot v(R)/T$. So let us first take a closer look at this inner product. p is the four-momentum of the parton, and $v(R)$ is the (dimensionless) velocity vector of the parton flow. To be precise,

$$v^\mu(R) = (\cosh \eta_L \cosh \eta_T, \sinh \eta_T \cos \phi, \sinh \eta_T \sin \phi, \sinh \eta_L \cosh \eta_T). \quad (3.10.3)$$

It is possible to fix $\eta_L = \eta$ (this is called a ‘‘Bjorken scenario’’). In this chapter, η_T (the transverse rapidity of the flow) will be considered to be independent of the azimuthal angle ϕ , just like the transverse distribution f mentioned earlier. Again, the independence of ϕ is a legitimate assumption only because we are studying central collisions here. In the next chapter, we will have to allow for a ϕ -dependence of the transverse flow. With the explicit shape (3.10.3) we can write out the inner product:

$$\begin{aligned} p \cdot v &= p^\mu v_\mu = p^0 v^0 - \mathbf{p} \cdot \mathbf{v} \\ &= m_T \cosh \eta_T (\cosh y \cosh \eta - \sinh y \sinh \eta) - p_T \sinh \eta_T (\cos \Phi \cos \phi + \sin \Phi \sin \phi) \\ &= m_T \cosh \eta_T \cosh(\eta - y) - p_T \sinh \eta_T \cos(\phi - \Phi). \end{aligned} \quad (3.10.4)$$

We see that if we want to approximate the Gaussian $e^{-\eta^2/2\Delta^2}$ by the constant function 1, a condition is that $\eta^2/2\Delta^2$ should be small when compared to $m_T \cosh \eta_T \cosh(\eta - y)$. We can ensure this by choosing to look at the region around zero rapidity ($y = 0$), since $\eta^2/2\Delta^2 \ll m_T \cosh \eta$.

Summarizing, we can write down the approximated expression for the parton phase space distribution that we will use in the following sections of this chapter, as

$$w(R; p) = \gamma e^{-p \cdot v(R)/T} \Theta(\rho_0 - \rho). \quad (3.10.5)$$

3.11 The parton spectrum at zero rapidity

For partons in thermal phase, the momentum distribution is

$$E_{\mathcal{Q}} \frac{dN_{\mathcal{Q}}^{th}}{d^3p} = g \int_{\Sigma} d\sigma_R \frac{p \cdot u(R)}{(2\pi)^3} w(R; p), \quad (3.11.1)$$

where the factor $g = 6$ (not to be confused with the metric tensor) counts the color and spin degeneracy of the parton. We want to express this momentum distribution in terms of the transverse momentum and the rapidity variable. To do this, we note that

$$d^3p = d^2p_T dp^z = d^2p_T d(m_T \sinh y) = m_T \cosh y d^2p_T dy. \quad (3.11.2)$$

In the case of zero rapidity, $y = 0$, the momentum of the parton in the z -direction is zero: $p_z = 0$. As a consequence, its energy equals its transverse mass:

$$E_{\mathcal{Q}}^2 = m^2 + p_T^2 + p_z^2 = m^2 + p_T^2 = m_T^2. \quad (3.11.3)$$

If we now combine equations (3.11.2) and (3.11.3), we can write the left side of (3.11.1) as

$$E_{\mathcal{Q}} \frac{dN_{\mathcal{Q}}^{th}}{d^3p} \Big|_{y=0} = \frac{E_{\mathcal{Q}}}{m_T \cosh y} \frac{dN_{\mathcal{Q}}^{th}}{d^2p_T dy} \Big|_{y=0} = \frac{dN_{\mathcal{Q}}^{th}}{d^2p_T dy} \Big|_{y=0}. \quad (3.11.4)$$

Now let us look at the *right* side of (3.11.1) at $y = 0$. For the parton phase space distribution we use expression (3.10.5). Furthermore, we can simply fill in the previously calculated expressions for the inner products $p \cdot v$ and $p \cdot u$:

$$\begin{aligned} g \int_{\Sigma} d\sigma_R \frac{p \cdot u(R)}{(2\pi)^3} w(R; p) &= g\gamma \int \tau \rho \, d\eta \, d\rho \, d\phi \frac{m_T \cosh \eta}{(2\pi)^3} e^{-(m_T \cosh \eta_T \cosh \eta - p_T \sinh \eta_T \cos(\phi - \Phi))/T} \Theta(\rho_0 - \rho) \\ &= \frac{g\gamma m_T \tau}{(2\pi)^3} \left(\int_0^{\rho_0} d\rho \right) \left(\int_0^{2\pi} d\phi e^{(p_T \sinh \eta_T \cos(\phi - \Phi))/T} \right) \left(\int_0^{\infty} d\eta \cosh \eta e^{-(m_T \cosh \eta_T \cosh \eta)/T} \right) \\ &= \frac{g\gamma m_T \tau \rho_0^2}{2(2\pi)^3} \left(\int_0^{2\pi} d\phi e^{(p_T \sinh \eta_T \cos(\phi - \Phi))/T} \right) \left(\int_0^{\infty} d\eta \cosh \eta e^{-(m_T \cosh \eta_T \cosh \eta)/T} \right). \end{aligned} \quad (3.11.5)$$

Because the integration over ϕ is from 0 to 2π , and the integrand is a 2π -periodic function, we may omit the $-\Phi$ in the cosine. To simplify our result, we can use the following definitions of modified Bessel functions of the first and second kind (cf. appendix A to find out why these are identical to the usual definitions of modified Bessel functions):

$$I_0(z) = \frac{1}{2\pi} \int_0^{2\pi} d\phi e^{z \cos \phi}; \quad (3.11.6)$$

$$K_1(z) = \frac{1}{2} \int_0^{\infty} d\eta \cosh \eta e^{-z \cosh \eta}. \quad (3.11.7)$$

So we end up with the parton spectrum

$$\frac{dN_{\mathcal{Q}}^{th}}{d^2p_T dy} \Big|_{y=0} = 2g\gamma m_T \frac{\tau A_T}{(2\pi)^3} I_0 \left(\frac{p_T \sinh \eta_T}{T} \right) K_1 \left(\frac{m_T \cosh \eta_T}{T} \right), \quad (3.11.8)$$

where A_T stands for the transverse area of the parton system, which is $\pi\rho_0^2$.

3.12 The ReCo meson spectrum at zero rapidity

To calculate the resulting meson momentum distribution at zero rapidity, we start from equation (3.7.13). As before in the case of partons, we can write the left side at zero rapidity as

$$E \frac{dN_M^{th}}{d^3P} \Big|_{y=0} = \frac{E}{M_T \cosh y} \frac{dN_M^{th}}{d^2P_T dy} \Big|_{y=0} = \frac{dN_M^{th}}{d^2P_T dy} \Big|_{y=0}. \quad (3.12.1)$$

In the right side of expression (3.7.13) there are two factors of the parton phase space distribution. For these we want to use the simplified expression for thermal partons (3.10.5).

However, we have to take great care in using the previously derived expression for $p \cdot v$, because that expression contains the transverse mass m_T of the parton with four-momentum p . But the right side of equation (3.7.13) contains the product

$$w(R; x\mathbf{P}) w(R; (1-x)\mathbf{P}) = \gamma^2 e^{-p_1 \cdot v(R)/T} e^{-p_2 \cdot v(R)/T}, \quad (3.12.2)$$

which means that in the exponent we encounter a sum of two *different* four-momenta, both multiplied by the same velocity vector:

$$p_1 \cdot v(R) + p_2 \cdot v(R). \quad (3.12.3)$$

Since the two partons have different transverse momenta (they can also have different masses, but here we will assume that both have mass m), their transverse masses will be different as well:

$$\begin{aligned} (m_T)_1 &= \sqrt{m^2 + p_{T1}^2} = \sqrt{m^2 + x^2 P_T^2}; \\ (m_T)_2 &= \sqrt{m^2 + p_{T2}^2} = \sqrt{m^2 + (1-x)^2 P_T^2}. \end{aligned} \quad (3.12.4)$$

Now that we are aware that the transverse masses of the two partons are not the same, we can safely use equation (3.10.4) to write

$$\begin{aligned} p_1 \cdot v(R) + p_2 \cdot v(R) &= \sqrt{m^2 + x^2 P_T^2} \cosh \eta_T \cosh \eta - x P_T \sinh \eta_T \cos(\phi - \Phi) \\ &+ \sqrt{m^2 + (1-x)^2 P_T^2} \cosh \eta_T \cosh \eta - (1-x) P_T \sinh \eta_T \cos(\phi - \Phi) \\ &= \mu_T(x, P_T) \cosh \eta_T \cosh \eta - P_T \sinh \eta_T \cos(\phi - \Phi), \end{aligned} \quad (3.12.5)$$

where $\mu_T^M(x, P_T) := \sqrt{m^2 + x^2 P_T^2} + \sqrt{m^2 + (1-x)^2 P_T^2}$.

Now we can work out the right hand side of equation (3.7.13):

$$\begin{aligned} &C_M \int_{\Sigma} \frac{d\sigma_R P \cdot u(R)}{(2\pi)^3} \int_0^1 dx w(R; x\mathbf{P}) |\phi_M(x)|^2 w(R; (1-x)\mathbf{P}) \\ &= C_M \gamma^2 \int \tau \rho d\eta d\rho d\phi \frac{M_T \cosh \eta}{(2\pi)^3} \\ &\quad \times \int_0^1 dx e^{-(\mu_T(x, P_T) \cosh \eta_T \cosh \eta - P_T \sinh \eta_T \cos(\phi - \Phi))/T} \Theta^2(\rho_0 - \rho) |\phi(x)|^2 \\ &= C_M M_T \tau \gamma^2 \left(\frac{\rho_0^2}{2(2\pi)^3} \right) \left(\int_0^{2\pi} d\phi e^{P_T \sinh \eta_T \cos(\phi - \Phi)/T} \right) \\ &\quad \times \left(\int_0^1 dx \int_0^\infty d\eta \cosh \eta e^{-\mu_T(x, P_T) \cosh \eta_T \cosh \eta/T} |\phi(x)|^2 \right) \\ &= C_M M_T \frac{\tau A_T}{(2\pi)^3} 2\gamma^2 I_0 \left(\frac{P_T \sinh \eta_T}{T} \right) \int_0^1 dx K_1 \left(\frac{\mu_T^M(x, P_T) \cosh \eta_T}{T} \right) |\phi(x)|^2. \end{aligned} \quad (3.12.6)$$

We can conclude that the momentum distribution for mesons of type M at zero meson rapidity now becomes

$$\left. \frac{dN_M}{d^2P_T dy} \right|_{y=0} = C_M M_T 2g \gamma^2 \frac{\tau A_T}{(2\pi)^3} I_0 \left(\frac{P_T \sinh \eta_T}{T} \right) \int_0^1 dx |\phi_M(x)|^2 k_M(x, P_T), \quad (3.12.7)$$

if we further define the function

$$k_M(x, P_T) := K_1 \left(\mu_T^M(x, P_T) \frac{\cosh \eta_T}{T} \right). \quad (3.12.8)$$

3.13 The ReCo baryon spectrum at zero rapidity

For baryons of type B , the derivation is completely analogous, starting from equation (3.7.14). Now we simply have to deal with *three* factors of the parton phase space distribution, and so we also get a sum of three inner products in the exponent:

$$w(R; x_1 \mathbf{P}) w(R; x_2 \mathbf{P}) w(R; x_3 \mathbf{P}) = \gamma^3 e^{-(p_1+p_2+p_3) \cdot v(R)/T}. \quad (3.13.1)$$

Calculation of the expression in the exponent is easy, as it closely resembles the calculation we did for the case of mesons:

$$\begin{aligned} (p_1 + p_2 + p_3) \cdot v(R) &= \mu_T^B(x_1, x_2, x_3, P_T) \cosh \eta_T \cosh \eta \\ &\quad - P_T \sinh \eta_T \cos(\phi - \Phi), \end{aligned} \quad (3.13.2)$$

where, predictably, $\mu_T^B(x_1, x_2, x_3, P_T) := \sqrt{m^2 + x_1^2 P_T^2} + \sqrt{m^2 + x_2^2 P_T^2} + \sqrt{m^2 + x_3^2 P_T^2}$. Here we have made use of the fact that the three momentum fractions x_1 , x_2 and x_3 add up to one, which is expressed in equation (3.7.14) by means of the delta function in the definition of the measure $\mathcal{D}x$.

Using exactly the same methods as in the derivation of formula (3.12.7), this immediately leads to

$$\left. \frac{dN_B}{d^2P_T dy} \right|_{y=0} = C_B M_T 2g \gamma^3 \frac{\tau A_T}{(2\pi)^3} I_0 \left(\frac{P_T \sinh \eta_T}{T} \right) \int \mathcal{D}x |\phi_B(x_1, x_2, x_3)|^2 k_B(x_1, x_2, x_3, P_T), \quad (3.13.3)$$

with the similar definition

$$k_B(x_1, x_2, x_3, P_T) = K_1 \left(\mu_T^B(x_1, x_2, x_3, P_T) \frac{\cosh \eta_T}{T} \right). \quad (3.13.4)$$

Chapter 4

Elliptic flow

4.1 Introduction

In this chapter we investigate the predictions that the recombination formalism of the previous chapter implies for the hadron elliptic flow as a function of transverse momentum. In order to calculate the elliptic flow, we use expressions for the hadron momentum distributions that are valid in the case of peripheral collisions.

4.1.1 The concept of elliptic flow

Let us look at the possibility that two heavy ion cores collide in a non-central collision. In that case, we can define a non-zero quantity called impact parameter (the symbol is b), which is simply the distance between the centers of the two colliding nuclei. We are interested in the initial shape of the overlap region in the plane transverse to the beam direction, because this will determine the shape of the hot and dense medium that exists immediately after the collision has taken place. It is clear that the intersection of the two individual circular regions will not be a circular one (see the picture in figure 4.1). Therefore, one should expect the parton phase space distribution in the hot and dense medium to depend on the azimuthal direction Φ of the momentum of the particle that is detected, because this direction determines the path length through the medium. This phenomenon is usually called “azimuthal anisotropy.”

Closely related to the azimuthal anisotropy that exists with non-central collisions, is a quantity called elliptic flow, usually denoted as v_2 . It can be seen as a measure for the amount of azimuthal anisotropy. It can be defined as the second moment of the Fourier expansion of a particle momentum distribution [12]:

$$\frac{dN}{d\Phi} = v_0(1 + 2v_1 \cos(\Phi) + 2v_2 \cos(2\Phi) + \dots), \quad (4.1.1)$$

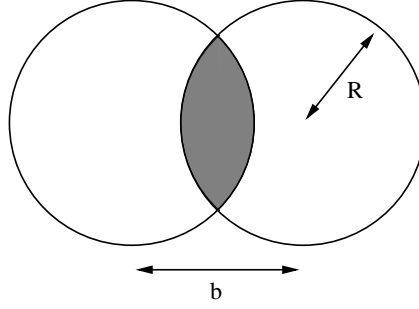


Figure 4.1: The geometry of a non-central collision of two ions. The parameters $w(b)$ and $l(b)$ that are used in this section are defined as half the width and half the height of the overlap region (the shaded region), respectively. So $l(b) = \sqrt{R^2 - (b/2)^2}$ and $w(b) = R - b/2$.

or as [3, 13, 21]¹

$$v_2(P_T) = \langle \cos(2\Phi) \rangle = \frac{\int d\Phi \cos(2\Phi) d^2N/dP_T^2}{\int d\Phi d^2N/dP_T^2}. \quad (4.1.2)$$

The idea behind these definitions is as follows. Because of the shape of the intersection region in figure 4.1, one would expect, for a given magnitude of the momentum, to detect more particles in the two horizontal directions ($\Phi = 0$ and $\Phi = \pi$), than in the two vertical directions ($\Phi = \pi/2$ and $\Phi = 3\pi/2$). In other words, one would expect the momentum distribution to show a certain amount of periodic behavior with a period of π radians with the highest values reached at $\Phi = 0$ and $\Phi = \pi$, and the lowest values reached at $\Phi = \pi/2$ and $\Phi = 3\pi/2$ (the expected shape for a fixed value of P_T is depicted in figure 4.2). The elliptic flow v_2 defined through equation (4.1.2), with values between 0 and 1, is a measure for how much a certain momentum distribution “looks like” a $\cos 2\Phi$.

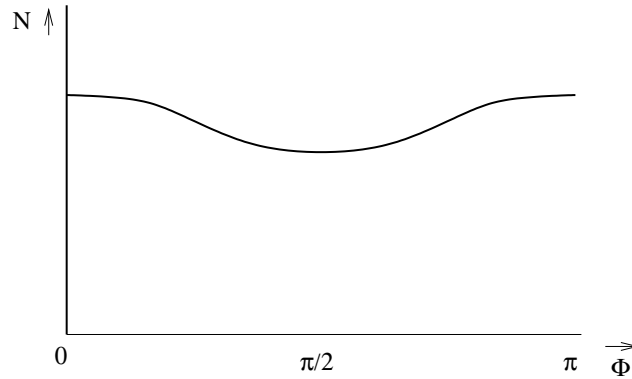


Figure 4.2: The expected momentum distribution as a function of the momentum angle Φ , for a fixed value of the transverse momentum.

¹Greco *et al.* [13, 21] use the seemingly different definition $v_2 = \langle (P_x^2 - P_y^2)/(P_x^2 + P_y^2) \rangle$. However, since $(P_x^2 - P_y^2)/(P_x^2 + P_y^2) = (P_x^2 - P_y^2)/P_T^2 = (P_x/P_T)^2 - (P_y/P_T)^2 = \cos^2 \Phi - \sin^2 \Phi = \cos 2\Phi$, their definition is in fact identical to (4.1.2).

4.1.2 Fragmentation and elliptic flow

We want to use the definition (4.1.2) to calculate the elliptic flow as a function of transverse momentum. The question is how exactly to make the hadron momentum distribution that we plug into (4.1.2) dependent on Φ . We should do this differently for hadrons that originate from fragmentation and for hadrons that originate from recombination. We assume that the former form from high transverse momentum partons (the perturbative tail of the parton spectrum), whereas we assume that the latter are made by coalescing partons with lower transverse momenta in a thermal phase. For hadrons that originate from fragmentation, we can calculate the Φ -dependence by calculating the energy loss that partons suffer when travelling through the hot and dense medium that exists immediately after the heavy ion collision (jet quenching). This energy loss depends on Φ in the following way:

$$\Delta p_T(b, p_T, \Phi) = \epsilon(b) \sqrt{p_T} \frac{\langle L \rangle}{R} (1 - \alpha \cos 2\Phi), \quad (4.1.3)$$

where $\langle L \rangle$ is the average path-length. The energy loss $\epsilon(b)$ can be parametrized as

$$\epsilon(b) = \epsilon_0 \frac{1 - e^{-(2R-b)/R}}{1 - e^{-2}}, \quad (4.1.4)$$

and the geometrical constant α is defined as

$$\alpha = \frac{w(b) - l(b)}{w(b) + l(b)}. \quad (4.1.5)$$

The momentum distribution for hadrons from fragmentation can then be calculated with the fragmentation formula (2.9.1), and the elliptic flow can be obtained by plugging the resulting expression into (4.1.2).

4.1.3 Recombination and elliptic flow

For elliptic flow from coalescence we have to use a different method. This is what we will be doing for the rest of this chapter: first we have to put in information about the anisotropic behavior of the partons. Subsequently, we can use our recombination model with this parton elliptic flow to derive what the elliptic flow of the resulting mesons and baryons will be.

Remember that we assumed that the involved partons are in thermal phase. After a collision, hydrodynamic expansion [16] of the anisotropic overlap zone of the two nuclei (the shaded region in figure 4.1) takes place. This expansion leads to a dependence of the transverse parton flow rapidity η_T on the azimuthal *space* angle ϕ . We model this dependence as

$$\eta_T(\phi) = \eta_T^0 (1 - f(p_T) \cos 2\phi), \quad (4.1.6)$$

in which $f(p_t)$ is the ‘‘amplitude’’ of anisotropy, for which we choose the *Ansatz*

$$f(p_T) = \frac{\alpha}{1 + (p_T/p_0)^2}. \quad (4.1.7)$$

The motivation for this choice for $f(p_T)$ is twofold. Firstly, we need a function that becomes small for large momenta, since we expect that faster partons will experience the anisotropy less than slower ones (the distance they travel through the medium is more or less fixed so their relative energy loss will be smaller). Secondly, the amplitude of anisotropy $f(p_T)$ should equal α for small values of the parton momentum.

The values of η_T^0 and p_0 in $\eta_T(\phi)$ can be obtained from comparison with results of experiments. For our calculations in the next chapter, we will use the values $\eta_T^0 = \text{arctanh}(0.55)$ and $p_0 = 1.1 \text{ GeV}/c$, obtained from PHENIX measurements [17].

4.2 Calculation of the parton elliptic flow

As a consequence of the ϕ -dependence of the transverse flow, the parton spectrum will actually also depend on the azimuthal *momentum* angle we introduced earlier, Φ . It is not difficult to see in precisely what way the parton spectrum at zero rapidity will now depend on Φ . The first part of the derivation is the same as in section 3.12, up to the point where the Φ -dependence dropped out, except that the η_T 's should be replaced by $\eta_T(\phi)$'s:

$$\left. \frac{dN_{\mathcal{Q}}^{th}}{d^2p_T dy} \right|_{y=0} = \frac{g\gamma m_T \tau \rho_0^2}{2(2\pi)^3} \int_0^{2\pi} d\phi e^{p_T \sinh \eta_T(\phi) \cos(\phi-\Phi)/T} \left(\int_0^\infty d\eta \cosh \eta e^{-m_T \cosh \eta_T(\phi) \cosh \eta/T} \right). \quad (4.2.1)$$

Now the $-\Phi$ in the cosine can't be dropped, because with the $\eta_T(\phi)$ in the exponent, we can no longer use a substitution of variables to get rid of all Φ s in the integrand. So, for our calculations in this section, we have to leave it like it is:

$$\left. \frac{dN_{\mathcal{Q}}^{th}}{d^2p_T dy} \right|_{y=0} = \frac{2g\gamma m_T \tau A_T}{(2\pi)^3} \frac{1}{4\pi} \int_0^{2\pi} d\phi e^{p_T \sinh \eta_T(\phi) \cos(\phi-\Phi)/T} 2K_1 \left(\frac{m_T \cosh \eta_T(\phi)}{T} \right). \quad (4.2.2)$$

From this expression, we want to calculate the parton elliptic flow. By definition,

$$v_2(p_T) = \langle \cos 2\Phi \rangle = \frac{\int_0^{2\pi} d\Phi \cos 2\Phi \left(\left. \frac{dN_{\mathcal{Q}}^{th}}{d^2p_T dy} \right|_{y=0} \right)}{\int_0^{2\pi} d\Phi \left(\left. \frac{dN_{\mathcal{Q}}^{th}}{d^2p_T dy} \right|_{y=0} \right)}. \quad (4.2.3)$$

First we calculate the numerator. The factor of $2g\gamma m_T \tau A_T / (2\pi)^3$ is omitted, since it will be cancelled by the denominator anyway. We are faced with both a ϕ -integral and a Φ -integral that we have to perform. To work out the Φ -integral, we can do a substitution of variables $\Phi' = \Phi - \phi$:

$$\begin{aligned} & \int_0^{2\pi} d\Phi \cos 2\Phi \left(\left. \frac{dN_{\mathcal{Q}}^{th}}{d^2p_T dy} \right|_{y=0} \right) \\ &= \frac{1}{4\pi} \int_0^{2\pi} d\phi \left(\int_0^{2\pi} d\Phi \cos 2\Phi e^{p_T \sinh \eta_T(\phi) \cos(\phi-\Phi)/T} \right) 2K_1 \left(\frac{m_T \cosh \eta_T(\phi)}{T} \right) \\ &= \frac{1}{2\pi} \int_0^{2\pi} d\phi \left(\int_0^{2\pi} d\Phi' \cos(2\Phi' + 2\phi) e^{p_T \sinh \eta_T(\phi) \cos \Phi'/T} \right) K_1 \left(\frac{m_T \cosh \eta_T(\phi)}{T} \right). \end{aligned} \quad (4.2.4)$$

At this point we can use the following identity:

$$\cos(2\Phi' + 2\phi) = \cos 2\Phi' \cos 2\phi - \sin 2\Phi' \sin 2\phi. \quad (4.2.5)$$

Consequently, we get two terms in the numerator of the parton elliptic flow, one with the cosines and one with the sines. However, the second term in (4.2.5) will not contribute, since

it leads to a 2π -periodic and odd term in the integrand:

$$\int_0^{2\pi} d\Phi' \sin 2\Phi' e^{p_T \sinh \eta_T(\phi) \cos \Phi'/T} = \int_{-\pi}^{\pi} d\Phi' \sin 2\Phi' e^{p_T \sinh \eta_T(\phi) \cos \Phi'/T} = 0. \quad (4.2.6)$$

So, for the numerator of (4.2.3) we are left with

$$\begin{aligned} & \frac{1}{2\pi} \int_0^{2\pi} d\phi \cos 2\phi \left(\int_0^{2\pi} d\Phi' \cos 2\Phi' e^{p_T \sinh \eta_T(\phi) \cos \Phi'/T} \right) K_1 \left(\frac{m_T \cosh \eta_T(\phi)}{T} \right) \\ &= \int_0^{2\pi} d\phi \cos 2\phi I_2 \left(\frac{p_T \sinh \eta_T(\phi)}{T} \right) K_1 \left(\frac{m_T \cosh \eta_T(\phi)}{T} \right). \end{aligned} \quad (4.2.7)$$

The calculation of the denominator of (4.2.3) using expression (3.11.8) is very straightforward. Again a factor of $2g\gamma m_T \tau A_T / (2\pi)^3$ is omitted because it would be cancelled by the numerator anyway. We write

$$\begin{aligned} \int_0^{2\pi} d\Phi \left(\frac{dN_{\mathcal{Q}}^{th}}{d^2p_T dy} \Big|_{y=0} \right) &= \frac{1}{4\pi} \int_0^{2\pi} d\phi \left(\int_0^{2\pi} d\Phi e^{p_T \sinh \eta_T(\phi) \cos(\phi-\Phi)/T} \right) 2K_1 \left(\frac{m_T \cosh \eta_T(\phi)}{T} \right) \\ &= \int_0^{2\pi} d\phi I_0 \left(\frac{p_T \sinh \eta_T(\phi)}{T} \right) K_1 \left(\frac{m_T \cosh \eta_T(\phi)}{T} \right). \end{aligned} \quad (4.2.8)$$

We finally arrive at a parton elliptic flow

$$v_2(p_T) = \frac{\int d\phi \cos 2\phi I_2(p_T \sinh \eta_T(\phi)/T) K_1(m_T \cosh \eta_T(\phi)/T)}{\int d\phi I_0(p_T \sinh \eta_T(\phi)/T) K_1(m_T \cosh \eta_T(\phi)/T)}. \quad (4.2.9)$$

4.3 Calculation of the meson elliptic flow

We want to compute the elliptic flow of mesons of type M through equation (4.1.2). This means we have to take into account the fact that the thermal parton phase space distribution that is featured in the parton spectrum, can no longer be assumed to be azimuthally isotropic. In the previous section we did this by making the transverse flow explicitly dependent on ϕ . This time, however, we keep $\eta_T = \eta_T^0$, but we account for the azimuthal anisotropy of the parton phase space distribution by using a factor of $[1 + 2v_2 \cos 2\Phi]$:

$$w^{a.i.}(R; p) = w(R; p) [1 + 2v_2(p_T) \cos 2\Phi], \quad (4.3.1)$$

with $w(R; p)$ from equation (3.10.5). Here, $v_2(p_T)$ is the *parton* elliptic flow. This method will enable us to connect the hadron elliptic flow to the parton elliptic flow, which can be measured experimentally. However, it must be said that expression (4.3.1) for the anisotropic

parton phase space distribution contains less information than the previously used expression with η_T as a function of ϕ . There are two reasons why:

1. The factor $[1 + 2v_2 \cos 2\Phi]$ is an approximation of the whole Fourier series, in which there could also be higher order terms featuring v_4 , etc. These higher harmonics have indeed been measured; for experimental results on v_4 by the STAR Collaboration, see Ref. [19].
2. Even if we take the full set of v_n 's into account, not all space-time information is contained. For a treatment of this problem, see for example reference [15].

Using the parton distribution (4.3.1), the spectrum of mesons of type M at zero rapidity from equation (3.7.13) becomes

$$\begin{aligned} \left. \frac{dN_M^{th}}{d^2P_T dy} \right|_{y=0} &= C_M \int_{\Sigma} \frac{d\sigma_R P \cdot u(R)}{(2\pi)^3} \int_0^1 dx w(R; x\mathbf{P}) [1 + 2v_2(xP_T) \cos 2\Phi] \\ &\quad \times |\phi_M(x)|^2 w(R; (1-x)\mathbf{P}) [1 + 2v_2((1-x)P_T) \cos 2\Phi]. \end{aligned} \quad (4.3.2)$$

Note that the momenta $x\mathbf{P}$ and $(1-x)\mathbf{P}$ share the same angle Φ , since both momenta are scalar multiples of the vector \mathbf{P} . For convenience, we define

$$\begin{aligned} V^M(x, \mathbf{P}) &:= [1 + 2v_2(xP_T) \cos 2\Phi] [1 + 2v_2((1-x)P_T) \cos 2\Phi] \\ &= 1 + 2[v_2(xP_T) + v_2((1-x)P_T)] \cos 2\Phi + 4v_2(xP_T) v_2((1-x)P_T) \cos^2 2\Phi \\ &= 1 + 2\sigma(x, P_T) \cos 2\Phi + 4\xi(x, P_T) \cos^2 2\Phi, \end{aligned} \quad (4.3.3)$$

in which

$$\sigma(x, P_T) = v_2(xP_T) + v_2((1-x)P_T), \quad (4.3.4)$$

and

$$\xi(x, P_T) = v_2(xP_T) v_2((1-x)P_T). \quad (4.3.5)$$

When we proceed to calculate the meson elliptic flow, the three terms in (4.3.3) will initially lead to three terms in the numerator of (4.1.2) and three terms in the denominator. Each of these six terms we will now calculate explicitly. As in the partonic case of the previous section, we first calculate the numerator of the meson elliptic flow, which is

$$\begin{aligned} \int_0^{2\pi} d\Phi \cos 2\Phi \left(\left. \frac{dN_M^{th}}{d^2P_T dy} \right|_{y=0} \right) &= C_M \int_0^{2\pi} d\Phi \cos 2\Phi \int_{\Sigma} \frac{d\sigma_R P \cdot u(R)}{(2\pi)^3} \\ &\quad \times \int_0^1 dx w(R; x\mathbf{P}) |\phi_M(x)|^2 w(R; (1-x)\mathbf{P}) V^M(x, \mathbf{P}). \end{aligned} \quad (4.3.6)$$

Again making use of the phase space distribution of thermal partons (3.10.5), the first term of $V^M(x, \mathbf{P})$ leads to a term

$$\begin{aligned} \frac{1}{4\pi} \int_0^{2\pi} d\Phi \cos 2\Phi \int_0^{2\pi} d\phi e^{P_T \sinh \eta_T \cos(\phi - \Phi)/T} \\ \times \int_0^1 dx \int_0^\infty d\eta \cosh \eta e^{-\mu_T^M(x, P_T) \cosh \eta_T \cosh \eta/T} |\phi_M(x)|^2 \end{aligned} \quad (4.3.7)$$

(We omit the factor of $C_M M_T \tau A_T 2\gamma^2 / (2\pi)^3$ in our calculations, since this factor will be cancelled by the denominator.) In principle, we are allowed to perform the ϕ -integral of the exponent before we perform the Φ -integral. But then the Φ -dependence in the $\cos(\phi - \Phi)$ disappears just as it did in section 3.11, since a 2π -periodic odd integrand is integrated over its whole period. This means that in all following calculations we can pretend that the $-\Phi$ in the $\cos(\phi - \Phi)$ is not there, which will lead to the presence of the simplest modified Bessel function $I_0(p_t \sinh \eta_T / T)$ in every term of both the numerator and the denominator of the hadron elliptic flow. We write (4.3.13) as

$$\frac{1}{4\pi} \left(\int_0^{2\pi} d\Phi \cos 2\Phi \right) 2\pi I_0 \left(\frac{P_T \sinh \eta_T}{T} \right) \int_0^1 dx 2k_M(x, P_T) |\phi_M(x)|^2, \quad (4.3.8)$$

but $\int_0^{2\pi} d\Phi \cos 2\Phi = 0$, so this whole first term vanishes.

The second term of (4.3.3), on the other hand, does make a non-zero contribution to the numerator of (4.1.2):

$$\begin{aligned} \frac{1}{4\pi} \int_0^{2\pi} d\Phi \cos^2 2\Phi \int_0^{2\pi} d\phi e^{P_T \sinh \eta_T \cos(\phi - \Phi)/T} \\ \times \int_0^1 dx 2\sigma(x, P_T) \int_0^\infty d\eta \cosh \eta e^{-\mu_T^M(x, P_T) \cosh \eta_T \cosh \eta/T} |\phi_M(x)|^2 \\ = \frac{1}{4\pi} \left(\int_0^{2\pi} d\Phi \cos^2 2\Phi \right) 2\pi I_0 \left(\frac{P_T \sinh \eta_T}{T} \right) \\ \times \int_0^1 dx 2\sigma(x, P_T) 2k_M(x, P_T) |\phi_M(x)|^2 \\ = \frac{1}{4\pi} \cdot \pi \cdot 2\pi I_0 \left(\frac{P_T \sinh \eta_T}{T} \right) \int_0^1 dx 2\sigma(x, P_T) 2k_M(x, P_T) |\phi_M(x)|^2 \\ = 2\pi I_0 \left(\frac{P_T \sinh \eta_T}{T} \right) \int_0^1 dx \sigma(x, P_T) k_M(x, P_T) |\phi_M(x)|^2. \end{aligned} \quad (4.3.9)$$

But the third term of (4.3.3) leads to a vanishing term again:

$$\begin{aligned}
& \frac{1}{4\pi} \int_0^{2\pi} d\Phi \cos^3 2\Phi \int_0^{2\pi} d\phi e^{P_T \sinh \eta_T \cos(\phi-\Phi)/T} \\
& \quad \times \int_0^1 dx 4\xi(x, P_T) \int_0^\infty d\eta \cosh \eta e^{-\mu_T^M(x, P_T) \cosh \eta_T \cosh \eta/T} |\phi_M(x)|^2 \\
& = \frac{1}{4\pi} \left(\int_0^{2\pi} d\Phi \cos^3 2\Phi \right) 2\pi I_0 \left(\frac{P_T \sinh \eta_T}{T} \right) \\
& \quad \times \int_0^1 dx 4\xi(x, P_T) 2k_M(x, P_T) |\phi_M(x)|^2 = 0, \quad (4.3.10)
\end{aligned}$$

since $\int_0^{2\pi} d\Phi \cos^3 2\Phi = 0$. So the total numerator of (4.1.2) for mesons is simply given by the contribution that we calculated from the $\cos^2 2\Phi$ -term:

$$2\pi I_0 \left(\frac{P_T \sinh \eta_T}{T} \right) \int_0^1 dx \sigma(x, P_T) k_M(x, P_T) |\phi_M(x)|^2. \quad (4.3.11)$$

The denominator of (4.1.2) for mesons is

$$\begin{aligned}
& \int_0^\pi d\Phi \left(\frac{dN_M^{th}}{d^2 P_T dy} \Big|_{y=0} \right) = C_M \int_0^{2\pi} d\Phi \int_\Sigma \frac{d\sigma_R P \cdot u(R)}{(2\pi)^3} \\
& \quad \times \int_0^1 dx w(R; x\mathbf{P}) |\phi_M(x)|^2 w(R; (1-x)\mathbf{P}) V^M(x, \mathbf{P}). \quad (4.3.12)
\end{aligned}$$

The first term of (4.3.3) immediately leads to the first denominator-term

$$\begin{aligned}
& \frac{1}{4\pi} \int_0^{2\pi} d\Phi \int_0^{2\pi} d\phi e^{P_T \sinh \eta_T \cos(\phi-\Phi)/T} \int_0^1 dx \int_0^\infty d\eta \cosh \eta e^{-\mu_T^M(x, P_T) \cosh \eta_T \cosh \eta/T} |\phi_M(x)|^2 \\
& \quad = 2\pi I_0 \left(\frac{P_T \sinh \eta_T(\phi)}{T} \right) \int_0^1 dx k_M(x, P_T) |\phi_M(x)|^2. \quad (4.3.13)
\end{aligned}$$

The second term of (4.3.3) leads to a vanishing term:

$$\begin{aligned}
& \frac{1}{4\pi} \left(\int_0^{2\pi} d\Phi \cos 2\Phi \right) \int_0^{2\pi} d\phi e^{P_T \sinh \eta_T \cos(\phi-\Phi)/T} \\
& \quad \times \int_0^1 dx 2\sigma(x, P_T) \int_0^\infty d\eta \cosh \eta e^{-\mu_T^M(x, P_T) \cosh \eta_T \cosh \eta/T} |\phi_M(x)|^2 \\
& \quad = 0 \quad (4.3.14)
\end{aligned}$$

Finally, the third term of (4.3.3) leads to the following contribution to the denominator of (4.1.2):

$$\begin{aligned}
& \frac{1}{4\pi} \left(\int_0^{2\pi} d\Phi \cos^2 2\Phi \right) \int_0^{2\pi} d\phi e^{P_T \sinh \eta_T \cos(\phi-\Phi)/T} \\
& \quad \times \int_0^1 dx 4\xi(x, P_T) \int_0^\infty d\eta \cosh \eta e^{-\mu_T^M(x, P_T) \cosh \eta_T \cosh \eta/T} |\phi_M(x)|^2 \\
& = \frac{1}{4\pi} \cdot \pi \cdot 2\pi I_0 \left(\frac{P_T \sinh \eta_T}{T} \right) \int_0^1 dx 4\xi(x, P_T) 2k_M(x, P_T) |\phi_M(x)|^2 \\
& = 4\pi I_0 \left(\frac{P_T \sinh \eta_T}{T} \right) \int_0^1 dx \xi(x, P_T) k_M(x, P_T) |\phi_M(x)|^2. \quad (4.3.15)
\end{aligned}$$

So the denominator of the meson elliptic flow is

$$2\pi I_0 (P_T \sinh \eta_T(\phi)/T) \int dx |\phi_M(x)|^2 [1 + 2\xi(x, P_T)] k_M(x, P_T). \quad (4.3.16)$$

We end up with

$$\begin{aligned}
v_2^M(P_T) &= \frac{2\pi I_0 (P_T \sinh \eta_T(\phi)/T) \int dx |\phi_M(x)|^2 \sigma(x, P_T) k_M(x, P_T)}{2\pi I_0 (P_T \sinh \eta_T(\phi)/T) \int dx |\phi_M(x)|^2 [1 + 2\xi(x, P_T)] k_M(x, P_T)} \\
&= \frac{\int dx |\phi_M(x)|^2 [v_2(xP_T) + v_2((1-x)P_T)] k_M(x, P_T)}{\int dx |\phi_M(x)|^2 [1 + 2v_2(xP_T)v_2((1-x)P_T)] k_M(x, P_T)}. \quad (4.3.17)
\end{aligned}$$

4.4 Calculation of the baryon elliptic flow

Of course we also want to know the elliptic flow for baryons. The calculation follows the same steps as the one for mesons. We start from expression (3.7.14), which contains three factors of the parton phase space distribution w . We make these azimuthally anisotropic again by replacing all three of these factors by

$$w^{\text{a.i.}}(R; p) = w(R; p) [1 + 2v_2(p_T) \cos 2\Phi], \quad (4.4.1)$$

with the appropriate momenta. The result is

$$\begin{aligned}
\left. \frac{dN_B^{\text{th}}}{d^2 P_T dy} \right|_{y=0} &= C_B \int_\Sigma \frac{d\sigma_R P \cdot u(R)}{(2\pi)^3} \int \mathcal{D}x_i w(R; x_1 \mathbf{P}) [1 + 2v_2(x_1 P_T) \cos 2\Phi] \\
& \quad \times w(R; x_2 \mathbf{P}) [1 + 2v_2(x_2 P_T) \cos 2\Phi] w(R; x_3 \mathbf{P}) [1 + 2v_2(x_3 P_T) \cos 2\Phi] |\phi_B(x_1, x_2, x_3)|^2. \quad (4.4.2)
\end{aligned}$$

Analogous to V^M in the previous section, we define²

$$\begin{aligned} V^B(x_i, \mathbf{P}) &= [1 + 2v_2(x_1 P_T) \cos 2\Phi] [1 + 2v_2(x_2 P_T) \cos 2\Phi] [1 + 2v_2(x_3 P_T) \cos 2\Phi] \\ &= 1 + 2\zeta(x_i, P_T) \cos 2\Phi + 4\vartheta(x_i, P_T) \cos^2 2\Phi + 8\chi(x_i, P_T) \cos^3 2\Phi, \end{aligned} \quad (4.4.3)$$

where

$$\begin{aligned} \zeta(x_i, P_T) &= v_2(x_1 P_T) + v_2(x_2 P_T) + v_2(x_3 P_T), \\ \vartheta(x_i, P_T) &= v_2(x_1 P_T)v_2(x_2 P_T) + v_2(x_1 P_T)v_2(x_3 P_T) + v_2(x_2 P_T)v_2(x_3 P_T), \text{ and} \\ \chi(x_i, P_T) &= v_2(x_1 P_T)v_2(x_2 P_T)v_2(x_3 P_T). \end{aligned} \quad (4.4.4)$$

The numerator of the baryon elliptic flow is then

$$\begin{aligned} \int_0^{2\pi} d\Phi \cos 2\Phi \left(\frac{dN_B^{th}}{d^2 P_T dy} \Big|_{y=0} \right) &= C_B \int_0^{2\pi} d\Phi \cos 2\Phi \int_{\Sigma} \frac{d\sigma_R P \cdot u(R)}{(2\pi)^3} \\ &\times \int \mathcal{D}x w(R; x_1 \mathbf{P}) w(R; x_2 \mathbf{P}) w(R; x_3 \mathbf{P}) |\phi_B(x_i)|^2 V^B(x_i, \mathbf{P}). \end{aligned} \quad (4.4.5)$$

The first term of $V^B(x_i, \mathbf{P})$ leads to a vanishing term since $\int_0^{2\pi} d\Phi \cos 2\Phi = 0$:

$$\begin{aligned} \frac{1}{4\pi} \left(\int_0^{2\pi} d\Phi \cos 2\Phi \right) \int_0^{2\pi} d\phi e^{P_T \sinh \eta_T \cos(\phi - \Phi)/T} \\ \times \int \mathcal{D}x \int_0^{\infty} d\eta \cosh \eta e^{-\mu_T^B(x_i, P_T) \cosh \eta_T \cosh \eta/T} |\phi_B(x_i)|^2 = 0. \end{aligned} \quad (4.4.6)$$

(Again, we omit all factors of $C_B M_T \tau A_T 2\gamma^3 / (2\pi)^3$ in our calculations) The second term of (4.4.3) does make a non-zero contribution to the numerator of the baryon elliptic flow:

$$\begin{aligned} \frac{1}{4\pi} \left(\int_0^{2\pi} d\Phi \cos^2 2\Phi \right) \int_0^{2\pi} d\phi e^{P_T \sinh \eta_T \cos(\phi - \Phi)/T} \\ \times \int \mathcal{D}x 2\zeta(x_i, P_T) \int_0^{\infty} d\eta \cosh \eta e^{-\mu_T^B(x_i, P_T) \cosh \eta_T \cosh \eta/T} |\phi_B(x_i)|^2 \\ = \frac{1}{4\pi} \cdot \pi \cdot 2\pi I_0 \left(\frac{P_T \sinh \eta_T}{T} \right) \int \mathcal{D}x 2\zeta(x_i, P_T) 2k_B(x_i, P_T) |\phi_B(x_i)|^2 \\ = 2\pi I_0 \left(\frac{P_T \sinh \eta_T}{T} \right) \int \mathcal{D}x \zeta(x_i, P_T) k_B(x_i, P_T) |\phi_B(x_i)|^2. \end{aligned} \quad (4.4.7)$$

²To keep things from looking too complicated, we use the shorthand notation $x_i := x_1, x_2, x_3$ throughout this section. No summation is intended if an expression contains more than one x_i .

But the third term of (4.4.3) leads to a vanishing term again:

$$\begin{aligned} & \frac{1}{4\pi} \int_0^{2\pi} d\Phi \cos^3 2\Phi \int_0^{2\pi} d\phi e^{P_T \sinh \eta_T \cos(\phi-\Phi)/T} \\ & \quad \times \int \mathcal{D}x \, 4\xi(x_i, P_T) \int_0^\infty d\eta \cosh \eta e^{-\mu_T^B(x_i, P_T) \cosh \eta_T \cosh \eta/T} |\phi_B(x_i)|^2 \\ & = 0, \end{aligned} \quad (4.4.8)$$

since $\int_0^{2\pi} d\Phi \cos^3 2\Phi = 0$. The fourth and final term in (4.4.3) results in a non-zero contribution of

$$\begin{aligned} & \frac{1}{4\pi} \left(\int_0^{2\pi} d\Phi \cos^4 2\Phi \right) \int_0^{2\pi} d\phi e^{P_T \sinh \eta_T \cos(\phi-\Phi)/T} \\ & \quad \times \int \mathcal{D}x \, 8\chi(x_i, P_T) \int_0^\infty d\eta \cosh \eta e^{-\mu_T^B(x_i, P_T) \cosh \eta_T \cosh \eta/T} |\phi_B(x_i)|^2 \\ & = \frac{1}{4\pi} \cdot \frac{3\pi}{4} \cdot 2\pi I_0 \left(\frac{P_T \sinh \eta_T}{T} \right) \int \mathcal{D}x \, 8\chi(x_i, P_T) 2k_B(x_i, P_T) |\phi_B(x_i)|^2 \\ & = 6\pi I_0 \left(\frac{P_T \sinh \eta_T}{T} \right) \int \mathcal{D}x \, \chi(x_i, P_T) k_B(x_i, P_T) |\phi_B(x_i)|^2. \end{aligned} \quad (4.4.9)$$

So the total numerator of (4.1.2) for baryons is given by the sum of the two non-zero contributions (4.4.7) and (4.4.9):

$$2\pi I_0 \left(\frac{P_T \sinh \eta_T}{T} \right) \int \mathcal{D}x \, [\zeta(x_i, P_T) + 3\chi(x_i, P_T)] k_B(x_i, P_T) |\phi_B(x_i)|^2. \quad (4.4.10)$$

The denominator of (4.1.2) for baryons is

$$\begin{aligned} & \int_0^\pi d\Phi \left(\frac{dN_B^{th}}{d^2 P_T dy} \Big|_{y=0} \right) = C_B \int_0^{2\pi} d\Phi \int_\Sigma \frac{d\sigma_R P \cdot u(R)}{(2\pi)^3} \\ & \quad \times \int \mathcal{D}x \, w(R; x_1 \mathbf{P}) w(R; x_2 \mathbf{P}) w(R; x_3 \mathbf{P}) |\phi_B(x_i)|^2 V^B(x_i, \mathbf{P}). \end{aligned} \quad (4.4.11)$$

The first term of (4.4.3) immediately leads to the first denominator-term

$$\begin{aligned} & \frac{1}{4\pi} \left(\int_0^{2\pi} d\Phi \right) \int_0^{2\pi} d\phi e^{P_T \sinh \eta_T \cos(\phi-\Phi)/T} \int \mathcal{D}x \int_0^\infty d\eta \cosh \eta e^{-\mu_T^B(x_i, P_T) \cosh \eta_T \cosh \eta/T} |\phi_B(x_i)|^2 \\ & = 2\pi I_0 \left(\frac{P_T \sinh \eta_T(\phi)}{T} \right) \int \mathcal{D}x \, k_B(x_i, P_T) |\phi_B(x_i)|^2. \end{aligned} \quad (4.4.12)$$

The second term of (4.4.3) leads to a vanishing term:

$$\begin{aligned} & \frac{1}{4\pi} \left(\int_0^{2\pi} d\Phi \cos 2\Phi \right) \int_0^{2\pi} d\phi e^{P_T \sinh \eta_T \cos(\phi-\Phi)/T} \\ & \quad \times \int \mathcal{D}x \, 2\zeta(x_i, P_T) \int_0^\infty d\eta \cosh \eta e^{-\mu_T^B(x_i, P_T) \cosh \eta_T \cosh \eta/T} |\phi_B(x_i)|^2 \\ & = 0. \end{aligned} \quad (4.4.13)$$

The third term of (4.4.3) leads to the following contribution to the denominator of (4.1.2):

$$\begin{aligned} & \frac{1}{4\pi} \left(\int_0^{2\pi} d\Phi \cos^2 2\Phi \right) \int_0^{2\pi} d\phi e^{P_T \sinh \eta_T \cos(\phi-\Phi)/T} \\ & \quad \times \int \mathcal{D}x \, 4\vartheta(x_i, P_T) \int_0^\infty d\eta \cosh \eta e^{-\mu_T^B(x_i, P_T) \cosh \eta_T \cosh \eta/T} |\phi_B(x_i)|^2 \\ & = \frac{1}{4\pi} \cdot \pi \cdot 2\pi I_0 \left(\frac{P_T \sinh \eta_T}{T} \right) \int \mathcal{D}x \, 4\vartheta(x_i, P_T) \, 2k_B(x_i, P_T) |\phi_B(x_i)|^2 \\ & = 4\pi I_0 \left(\frac{P_T \sinh \eta_T}{T} \right) \int \mathcal{D}x \, \vartheta(x_i, P_T) \, k_B(x_i, P_T) |\phi_B(x_i)|^2. \end{aligned} \quad (4.4.14)$$

Finally, the fourth and final term of (4.4.3) leads to a vanishing term:

$$\begin{aligned} & \frac{1}{4\pi} \left(\int_0^{2\pi} d\Phi \cos^3 2\Phi \right) \int_0^{2\pi} d\phi e^{P_T \sinh \eta_T \cos(\phi-\Phi)/T} \\ & \quad \times \int \mathcal{D}x \, 8\chi(x_i, P_T) \int_0^\infty d\eta \cosh \eta e^{-\mu_T^B(x_i, P_T) \cosh \eta_T \cosh \eta/T} |\phi_B(x_i)|^2 \\ & = 0. \end{aligned} \quad (4.4.15)$$

So the total denominator of the baryon elliptic flow is

$$2\pi I_0 (P_T \sinh \eta_T/T) \int \mathcal{D}x \, |\phi_B(x_i)|^2 [1 + 2\vartheta(x_i, P_T)] k_B(x_i, P_T). \quad (4.4.16)$$

We conclude that the elliptic flow for baryons is given by

$$\begin{aligned} v_2^B(P_T) &= \frac{2\pi I_0 (P_T \sinh \eta_T/T) \int \mathcal{D}x \, |\phi_B(x_i)|^2 [\zeta(x_i, P_T) + 3\chi(x_i, P_T)] k_B(x_i, P_T)}{2\pi I_0 (P_T \sinh \eta_T/T) \int \mathcal{D}x \, |\phi_B(x_i)|^2 [1 + 2\vartheta(x_i, P_T)] k_B(x_i, P_T)} \\ &= \frac{\int \mathcal{D}x \, |\phi_B(x_1, x_2, x_3)|^2 [v_2(x_1 P_T) + v_2(x_2 P_T) + v_2(x_3 P_T) + 3v_2(x_1 P_T)v_2(x_2 P_T)v_2(x_3 P_T)] k_B(x_i, P_T)}{\int \mathcal{D}x \, |\phi_B(x_1, x_2, x_3)|^2 [1 + 2(v_2(x_1 P_T)v_2(x_2 P_T) + v_2(x_1 P_T)v_2(x_3 P_T) + v_2(x_2 P_T)v_2(x_3 P_T))] k_B(x_i, P_T)}. \end{aligned} \quad (4.4.17)$$

4.5 Quark number scaling

To get further insight into the results of our calculations, we make use again of the approximation that the longitudinal distribution amplitudes $\phi_M(x)$ and $\phi_B(x_1, x_2, x_3)$ are very narrow and centered around the expected momentum fractions of $x = 1/2$ for mesons and $x_1 = x_2 = x_3 = 1/3$ for baryons (see section 3.8):

$$|\phi_M(x)|^2 = \delta\left(x - \frac{1}{2}\right), \quad (4.5.1)$$

$$|\phi_B(x_1, x_2, x_3)|^2 = \delta\left(x_1 - \frac{1}{3}\right) \delta\left(x_2 - \frac{1}{3}\right). \quad (4.5.2)$$

With these approximations, the hadron elliptic flow immediately becomes

$$v_2^M(P_T) = \frac{v_2(\frac{1}{2}P_T) + v_2(\frac{1}{2}P_T)}{1 + 2v_2(\frac{1}{2}P_T)v_2(\frac{1}{2}P_T)} = \frac{2v_2(\frac{1}{2}P_T)}{1 + 2v_2(\frac{1}{2}P_T)^2} \quad (4.5.3)$$

for mesons, and

$$\begin{aligned} v_2^B(P_T) &= \frac{v_2(\frac{1}{3}P_T) + v_2(\frac{1}{3}P_T) + v_2(\frac{1}{3}P_T) + 3v_2(\frac{1}{3}P_T)v_2(\frac{1}{3}P_T)v_2(\frac{1}{3}P_T)}{1 + 2(v_2(\frac{1}{3}P_T)v_2(\frac{1}{3}P_T) + v_2(\frac{1}{3}P_T)v_2(\frac{1}{3}P_T) + v_2(\frac{1}{3}P_T)v_2(\frac{1}{3}P_T))} \\ &= \frac{3v_2(\frac{1}{3}P_T) + 3v_2(\frac{1}{3}P_T)^3}{1 + 6v_2(\frac{1}{3}P_T)^2} \end{aligned} \quad (4.5.4)$$

for baryons.

Values of the parton elliptic flow are usually quite small (smaller than 0.1, see also section 5.2.1 and Ref. [3]), so we can neglect quadratic and higher-order terms. This leads to the famous quark number scaling law:

$$v_2^M(P_T) = 2v_2(P_T/2), \quad (4.5.5)$$

and

$$v_2^B(P_T) = 3v_2(P_T/3). \quad (4.5.6)$$

It can be summarized as

$$v_2^h(P_T) = nv_2(P_T/n), \quad (4.5.7)$$

where n is the number of valence quarks and anti-quarks that constitute the hadron of type h . In other words, the meson (baryon) elliptic flow is simply the sum of the elliptic flows of its two (three) constituents, where all two (three) parton elliptic flows are evaluated at the one half (one third) of the meson (baryon) transverse momentum, i.e. precisely the momentum that we assumed them to carry, through (4.5.1).

Note that we have derived this scaling law using an approximation with narrow longitudinal amplitudes $\phi_M(x)$ and $\phi_B(x_1, x_2, x_3)$. In the next chapter, we investigate (among other

things) whether or not this quark number scaling also holds for realistic, broad amplitudes. As mentioned in section 1.1, experimental results from PHENIX on elliptic flow have indeed shown that this scaling law is obeyed by pions and protons, down to P_T -values of about 500 MeV/ c (see figure 1.1). Recent experiments show that it is also obeyed by other mesons, such as the ϕ -meson [20].

4.6 Including fragmentation

We have calculated the elliptic flow that results from recombination processes. If, for a certain value of the transverse hadron momentum, we also want to include the elliptic flow of hadrons that originate from *fragmentation*, we would ideally use the total hadron spectrum $dN^{total}/d^2P_T = dN^R/d^2P_T + dN^F/d^2P_T$ in the definition of elliptic flow, expression (4.1.2). However, in practise it is more convenient to use the purely ReCo elliptic flow and the purely fragmentation elliptic flow. Of course we cannot just add them up to obtain the total elliptic flow; we need a sensible weight factor. In order to achieve roughly the same result as we would get by using $dN^{total}/d^2P_T = dN^R/d^2P_T + dN^F/d^2P_T$ in (4.1.2), we have to define the weight factor as

$$r(P_T) = \frac{dN^R/d^2P_T}{dN^R/d^2P_T + dN^F/d^2P_T}. \quad (4.6.1)$$

The total elliptic flow is then given by the weighted sum of the ReCo and fragmentation elliptic flows:

$$v_2(P_T) = r(P_T)v_2^R(P_T) + (1 - r(P_T))v_2^F(P_T). \quad (4.6.2)$$

Chapter 5

A graphic look at the results of the ReCo formalism

5.1 Introduction

Because most of the formulas that we derived in the previous two chapters contain rather complicated elements (such as modified Bessel functions and integrations that have yet to be executed), they are not easy to appreciate in an intuitive way. Therefore, it is useful to employ numerical methods to obtain concrete results. As we will show in this final chapter, plots of the derived expressions for the ReCo spectra and elliptic flows offer much insight in the physical implications of our recombination model.

A note on the constants in the formulas: for all our numerical calculations in this chapter we have used the values $g = 6$, $\gamma = 1$, $\rho_0 = 9$ fm, $\eta_T^0 = \text{arctanh}(0.55)$, $p_0 = 1.1$ GeV/ c , $C_\pi = 1$, $C_p = 2$, $m = 260$ MeV, $M_\pi = 139.6$ MeV and $M_p = 938$ MeV.

5.2 Momentum distributions

5.2.1 Partons

We start with a look at the parton spectrum from equation (3.11.8). A plot with a logarithmic vertical scale is shown in figure 5.1¹. It shows the parton spectrum in the transverse momentum region where we expect recombination to be the dominant hadronization process (up to $p_T \approx 6$ GeV). Clearly, this parton spectrum closely resembles a thermal (exponential) distribution. This is hardly surprising, since we calculated the parton spectrum (3.11.8) from

¹We have divided every plotted momentum distribution in this chapter by 2π times the transverse parton or hadron momentum.

relation (3.11.1),

$$E_Q \frac{dN_Q^{th}}{d^3p} = g \int_{\Sigma} d\sigma_R \frac{p \cdot u(R)}{(2\pi)^3} w(R; p), \quad (5.2.1)$$

with an explicitly thermal parton phase space distribution $w(R; p) = \gamma e^{-p \cdot v(R)/T} \Theta(\rho_0 - \rho)$.

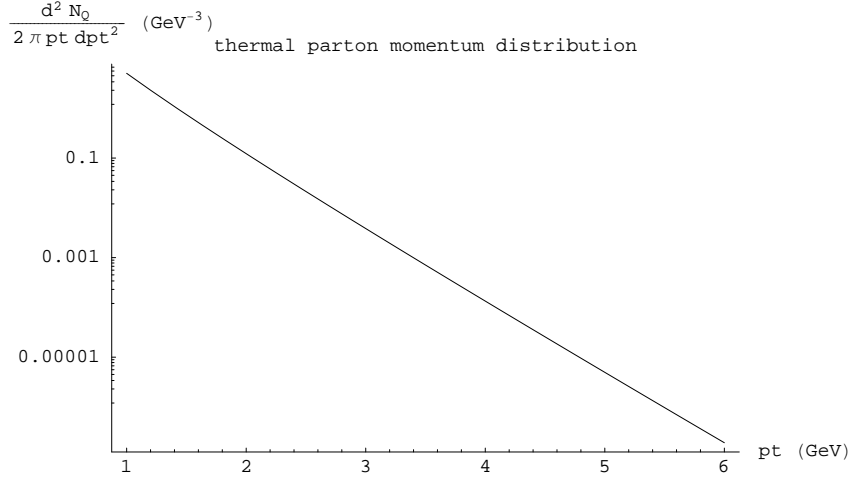


Figure 5.1: Transverse momentum distribution of partons at $T = 175$ GeV on a logarithmic scale.

5.2.2 Pions

Next, we turn to the pion spectrum, depicted in figure 5.2. It is a special case of expression (3.12.7):

$$\left. \frac{dN_\pi}{d^2P_T dy} \right|_{y=0} = C_\pi M_T 2g\gamma^2 \frac{\tau\pi\rho_0^2}{(2\pi)^3} I_0 \left(\frac{P_T \sinh \eta_T^0}{T} \right) \int_0^1 dx |\phi_\pi(x)|^2 k_\pi(x, P_T), \quad (5.2.2)$$

with

$$k_\pi(x, P_T) := K_1 \left(\left(\sqrt{m^2 + x^2 P_T^2} + \sqrt{m^2 + (1-x)^2 P_T^2} \right) \frac{\cosh \eta_T^0}{T} \right). \quad (5.2.3)$$

In figure 5.2, two lines are shown, corresponding to two different choices for the shape of the longitudinal amplitude $\phi_\pi(x)$. One is a shape which we will also refer to as the broad pion amplitude. It is maximal for $x = 1/2$ (equal light cone momentum fractions of the partons), but it does allow for some dispersion of the momenta:

$$\phi_\pi^{\text{broad}}(x) = \sqrt{30} x (1-x). \quad (5.2.4)$$

The resulting pion spectrum is the solid line in figure (5.2). Another informative choice is the delta function approximation, which we introduced in section 3.8. In this approximation, the

amplitude is so narrow that only equal light cone momentum fractions of 1/2 are allowed:

$$|\phi_{\pi}^{\text{narrow}}(x)|^2 = \delta\left(x - \frac{1}{2}\right). \quad (5.2.5)$$

The resulting pion spectrum if we plug this delta function into the general pion expression, is easily seen to be

$$\left. \frac{dN_{\pi}^{\text{narrow}}}{d^2 P_T dy} \right|_{y=0} = C_{\pi} M_T 2g\gamma^2 \frac{\tau\pi\rho_0^2}{(2\pi)^3} I_0\left(\frac{P_T \sinh \eta_T}{T}\right) K_1\left(\sqrt{4m_{\pi}^2 + P_T^2} \frac{\cosh \eta_T^0}{T}\right). \quad (5.2.6)$$

It is depicted as the dashed line in figure (5.2). Note that on this logarithmic scale, the two pion spectra almost coincide, especially for larger transverse momenta. More about the comparison between broad and narrow longitudinal amplitude after we have discussed the proton spectrum (figure 5.3).

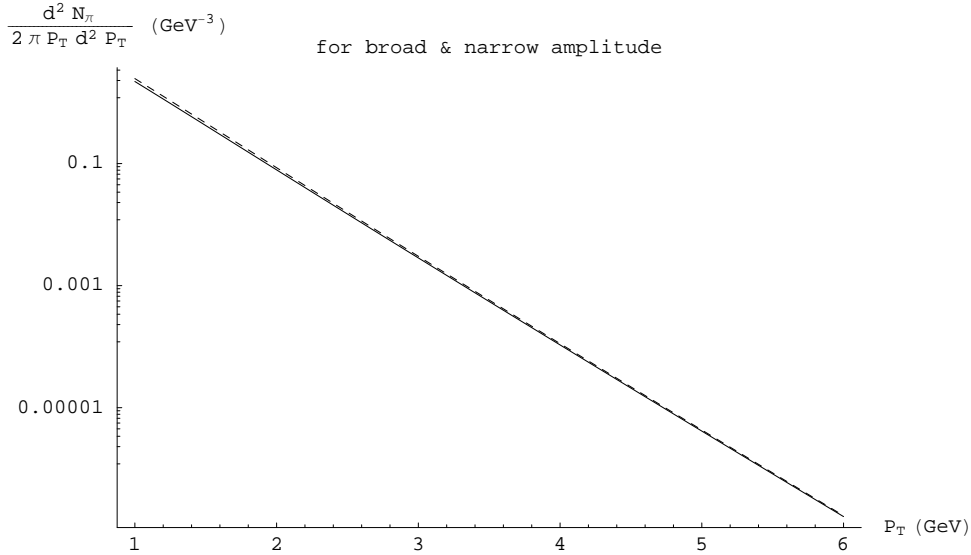


Figure 5.2: Transverse momentum distribution of pions. Shown are the results using a realistic, broad longitudinal amplitude (solid line) as well as the results using a narrow amplitude (dashed line).

5.2.3 Protons

For protons we make a similar distinction between a broad proton longitudinal amplitude and a narrow one. A properly normalized broad amplitude is

$$\phi_p^{\text{broad}}(x_1, x_2, x_3) = 12\sqrt{35} x_1 x_2 x_3. \quad (5.2.7)$$

We have used this amplitude in combination with the general proton spectrum that is given through equation (3.13.3) by

$$\left. \frac{dN_p}{d^2 P_T dy} \right|_{y=0} = C_p M_T 2g\gamma^3 \frac{\tau\pi\rho_0^2}{(2\pi)^3} I_0 \left(\frac{P_T \sinh \eta_T^0}{T} \right) \int \mathcal{D}x |\phi_p(x_1, x_2, x_3)|^2 k_p(x_1, x_2, x_3, P_T), \quad (5.2.8)$$

with

$$k_p(x_1, x_2, x_3, P_T) = K_1 \left(\left(\sqrt{m^2 + x_1^2 P_T^2} + \sqrt{m^2 + x_2^2 P_T^2} + \sqrt{m^2 + x_3^2 P_T^2} \right) \frac{\cosh \eta_T^0}{T} \right), \quad (5.2.9)$$

to obtain the solid line in figure 5.3. Just as in the pion case, we have also plotted the spectrum using a narrow amplitude approximation. The appropriate delta function amplitude is

$$|\phi_p^{\text{narrow}}(x_1, x_2, x_3)|^2 = \delta \left(x_1 - \frac{1}{3} \right) \delta \left(x_2 - \frac{1}{3} \right). \quad (5.2.10)$$

It leads to

$$\left. \frac{dN_p^{\text{narrow}}}{d^2 P_T dy} \right|_{y=0} = C_p M_T 2g\gamma^3 \frac{\tau\pi\rho_0^2}{(2\pi)^3} I_0 \left(\frac{P_T \sinh \eta_T^0}{T} \right) K_1 \left(\sqrt{9m^2 + P_T^2} \frac{\cosh \eta_T^0}{T} \right). \quad (5.2.11)$$

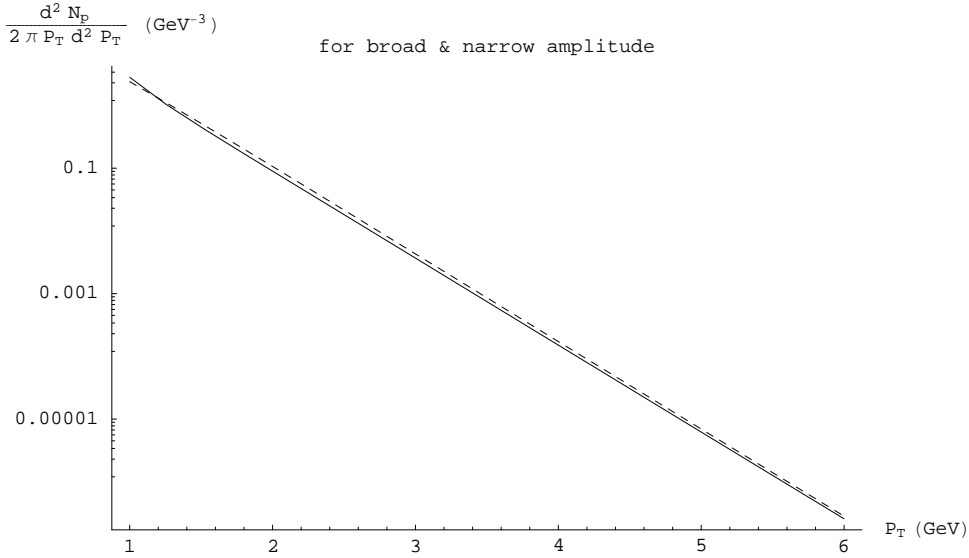


Figure 5.3: Transverse momentum distribution of protons. Shown are the results using a broad longitudinal amplitude (solid line) as well as the results using a narrow amplitude (dashed line).

Both proton spectra are shown in figure 5.3. Summarizing the first three plots, we see that in a recombination model the formed pions and protons almost exactly inherit the thermal behavior that we assumed of the coalescing partons. Figure 5.4 shows that for not too high P_T values the derived ReCo pion and proton spectrum closely resemble thermal spectra of $T = 300$ MeV, even though as input we used a thermal parton phase at $T = 175$ MeV.

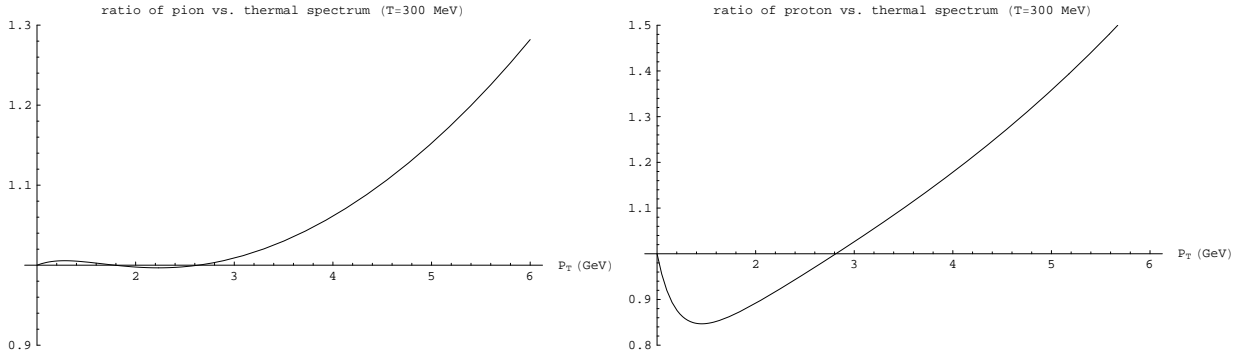


Figure 5.4: Ratio of the ReCo hadron spectrum and a thermal spectrum at $T = 300$ MeV for pions and protons, respectively.

5.2.4 Narrow vs. broad amplitude

On first sight there doesn't seem to be a big difference between the use of a narrow amplitude or a broad one. Upon closer inspection of figures 5.2 and 5.3 though, we see that the use of a narrow amplitude is not as good an approximation in the proton case as it was in the pion case. We can make this observation more clearly visible by plotting the relative difference of the spectra using broad and narrow amplitudes. We define this relative difference straightforwardly as

$$d(P_T) = \frac{\left. \frac{dN^{\text{broad}}}{d^2 P_T dy} \right|_{y=0} - \left. \frac{dN^{\text{narrow}}}{d^2 P_T dy} \right|_{y=0}}{\left. \frac{dN^{\text{broad}}}{d^2 P_T dy} \right|_{y=0}}. \quad (5.2.12)$$

We have plotted this fraction both for pions and for protons in figure 5.5. It shows us four important facts about the use of a delta function approximation for the longitudinal pion or proton amplitude:

1. deviations are significantly larger for protons than they are for pions;
2. the relative difference is mostly negative, meaning that the narrow amplitude approximation yields slightly too high results;
3. deviations are smaller than 20% for all transverse momenta larger than 1 GeV;
4. the relative difference is significant for small momenta; the narrow amplitude approximation becomes a good approximation for transverse hadron momenta larger than 6 GeV. This has to do with the fact that the problems that exist with the violation of energy conservation in recombination processes, are less important for large P_T [3, 8].

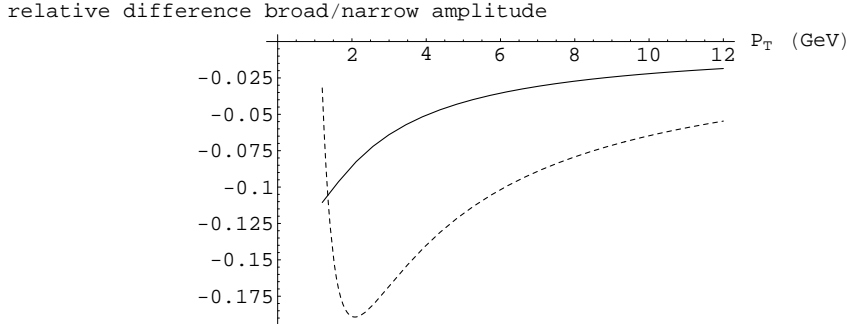


Figure 5.5: Relative difference between using a realistic, broad amplitude and a narrow (delta function) amplitude to calculate the hadron spectrum. This relative difference is shown for the pion spectrum (solid line) and for the proton spectrum (dashed line).

5.2.5 Pions vs. protons

We also plotted the pion spectrum and the proton spectrum together (figure 5.6), using only the broad amplitude spectra. In order to be able to compare their respective shapes, we have modified the normalization of the proton spectrum to make it assume the same value as the pion spectrum at $P_T = 1$ GeV. Apart from some differences at low P_T (caused by mass effects), it is striking that the two lines have almost the exact same slope. This can be understood directly from formulas (5.2.2) and (5.2.8): in principle, the transverse mass $M_T = \sqrt{M_h^2 + P_T^2}$ in the prefactors of both formulas makes up for a large part² of the difference between pions and protons, since $M_\pi = 139.6$ MeV and $M_p = 938$ MeV. But if the transverse hadron momentum becomes large when compared to the hadron mass M_h , the mass difference does not matter anymore since then we have $M_T \approx P_T$ for any hadron species. In other words, it follows from our ReCo model that, for high hadron momenta, there is almost no distinction between pions and protons (except in the normalization factor).

Of course, we can also compare the pion spectrum and the proton spectrum by looking at their ratio as a function of transverse hadron momentum. In figure 5.7, we see the calculated ReCo proton-to-pion ratio as a function of transverse hadron momentum. The most interesting line is the solid one, since it was made using the (more realistic) broad amplitudes (for protons as well as for pions). This time, we have deduced the missing normalization constant from a comparison of our pion and proton spectra and experimental data [18]. This means that the values of the ratio in figure 5.7 should be the real physical values. The most interesting part of this plot is for transverse momenta of roughly 4 – 6 GeV, where the shape of this

²Of course, the other differences are in the used longitudinal amplitudes and in the exponents in the definitions of k_π and k_p .

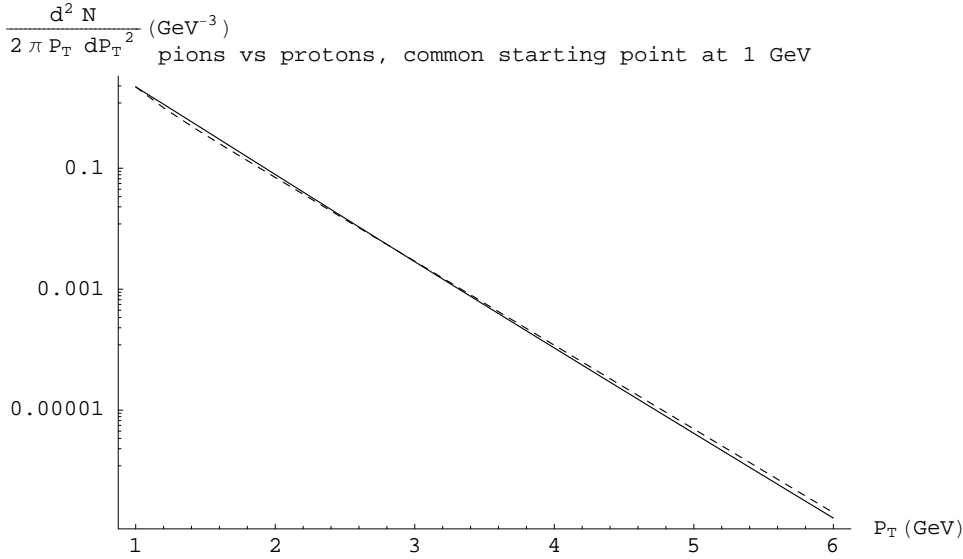


Figure 5.6: Pion spectrum (solid line) and proton spectrum (dashed line), both from a broad amplitude calculation. The normalization of the proton spectrum has been modified in such a way, that both spectra have the same starting point at $P_T = 1$ GeV.

ReCo proton-to-pion ratio more or less matches the experimental results from PHENIX [4]. Unfortunately, the predicted values in figure 5.7 are consistently too high, as they should be around 1. The matching with experimental data improves for higher momenta, when also fragmentation processes are taken into account [3]. Fragmentation predicts a proton-to-pion ratio of about 0.1, so it drags the recombination proton-to-pion ratio down in the momentum region where it is dominant.

It is sometimes argued that a recombination model naturally leads to a high proton-to-pion ratio. This view is usually inspired by the thermal shape of the parton spectrum, figure 5.1. The reasoning goes as follows: for a proton with a given value of P_T , one needs three partons, each with momentum $p_T \approx P_T/3$. For a *pion* with momentum P_T , one needs two partons of momentum $p_T \approx P_T/2$. That is, *each one of these two partons has a larger momentum than $P_T/3$* . Therefore, these two partons are lower down the slope of the parton spectrum than the proton-forming partons. In this way, we could conclude that we can estimate for any value of transverse momentum we get relatively many protons and few pions. However, we need to realize that in estimates of the hadron spectra we should use three or two factors of the parton spectrum. For the conclusion of the above reasoning to be valid, $d^2 N_Q / dp_T^2$ has to be sufficiently high-valued to ensure that indeed

$$\left(\frac{d^2 N_Q}{dp_T^2} \Big|_{p_T = \frac{P_T}{3}} \right)^3 > \left(\frac{d^2 N_Q}{dp_T^2} \Big|_{p_T = \frac{P_T}{2}} \right)^2. \quad (5.2.13)$$

But, as we mentioned in section 3.10, we have not taken a normalization factor of $w(p)$ into account, so our model really does not say anything about the numerical values of the derived

parton spectra; we really only have derived information about the dependence of the spectra on transverse momentum. This means that our recombination model does not guarantee that condition (5.2.13) is satisfied.

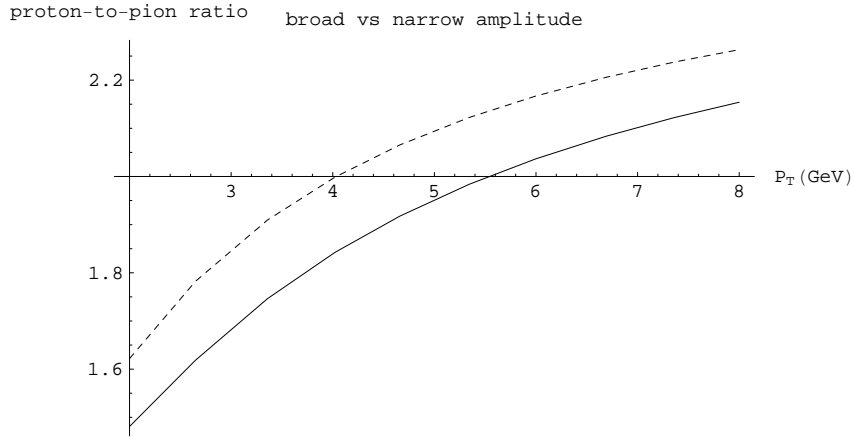


Figure 5.7: The ReCo proton-to-pion ratio, calculated from the separate proton and pion spectra. The solid line represents the proton-to-pion ratio using broad longitudinal amplitudes for both protons and pions. The dashed line shows the ratio resulting from a narrow amplitude calculation.

5.3 Elliptic flow and quark number scaling

5.3.1 Partons

In this section, it is convenient to work with a scaled impact parameter variable $\xi = b/2R$, instead of with the impact parameter itself. Clearly, ξ can run from 0, which means a central collision, to 1, which means an extremely peripheral collision. We rewrite the width $w(b)$ and length $l(b)$ of the intersection region in terms of ξ :

$$w = R - \frac{b}{2} = R \left(1 - \frac{b}{2R}\right) = R(1 - \xi), \text{ and} \quad (5.3.1)$$

$$l = \sqrt{R^2 - \left(\frac{b}{2}\right)^2} = R \sqrt{1 - \left(\frac{b}{2R}\right)^2} = R \sqrt{1 - \xi^2}. \quad (5.3.2)$$

In the resulting expression for α , the common factor of R drops out:

$$\alpha = \frac{w - l}{w + l} = \frac{1 - \xi - \sqrt{1 - \xi^2}}{1 - \xi + \sqrt{1 - \xi^2}}. \quad (5.3.3)$$

We start this section by looking at the parton elliptic flow (figure 5.8) that we calculated (equation (4.2.9)). Remember that we more or less put this information into the recombination model ourselves (which is why the plot carries the title “ReCo parton elliptic flow”, even though obviously no recombination processes take place). For example, the decreasing behavior (after the elliptic flow reaches its maximum) is something we forced through our choice for the function $f(p_T)$ (see section 4.1); we wanted to ensure that fast partons experience the anisotropy in the expansion less than slower ones. The elliptic flow increase at the start (from $p_T = 0$ up to $p_T \approx 2$ GeV) can simply be explained by the fact that there cannot be anisotropy for zero momentum partons.

Furthermore, it is informative to see that for increasing values of the (scaled) impact parameter we find larger azimuthal anisotropies. This could be expected, since a large impact parameter means a very peripheral collision and therefore a more significant anisotropy in the expansion.

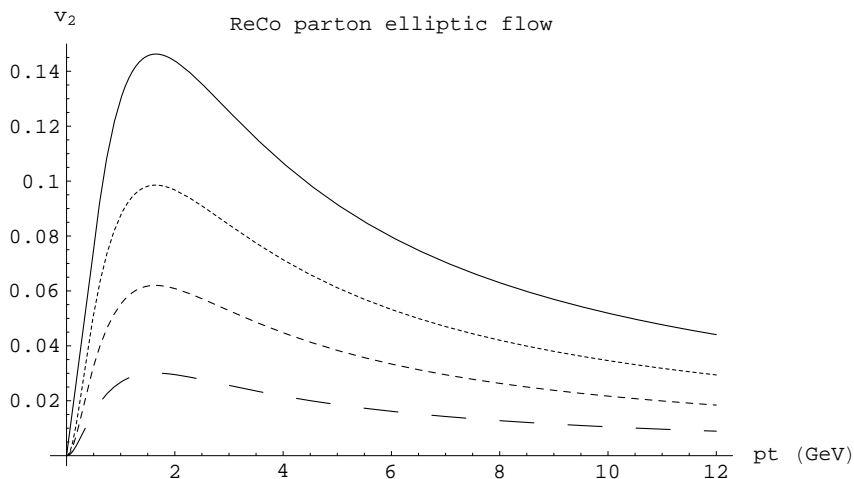


Figure 5.8: The parton elliptic flow for (from top to bottom) $\xi = 0.8$, $\xi = 0.6$, $\xi = 0.4$ and $\xi = 0.2$.

5.3.2 Pions

Let us find out what the pion elliptic flow in equation (4.3.17) looks like in a plot. It is pictured in figure 5.9 for $\xi = 0.4$, and in figure 5.10 for four values of the impact parameter. In the first of these two pictures, also the pion elliptic flow of equation (4.5.3), resulting from the use of the delta function amplitude, is shown. It reaches higher values than the more realistic (and more complicated) elliptic flow with broad amplitude. In other words, more momentum dispersion leads to a lower peak anisotropy. Comparing the narrow amplitude approximation in figure 5.9 with the parton elliptic flow at $\xi = 0.4$ in figure 5.8, leads to the observation that pions more or less seem to inherit the elliptic flow behavior of the coalescing

partons, apart from a factor of two. We will come back to this apparent scaling effect at the end of this chapter.

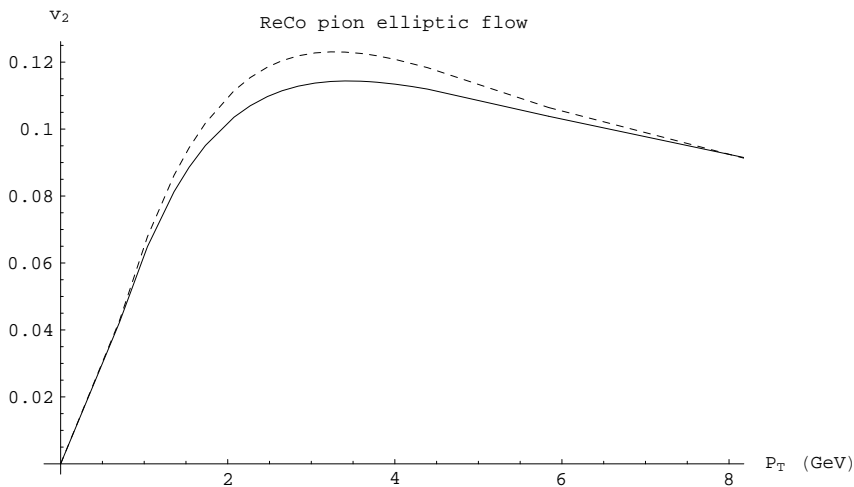


Figure 5.9: The pion elliptic flow at $\xi = 0.4$, resulting from equation (4.3.17) using a broad amplitude (solid line) and a narrow (delta function) amplitude (dashed line).

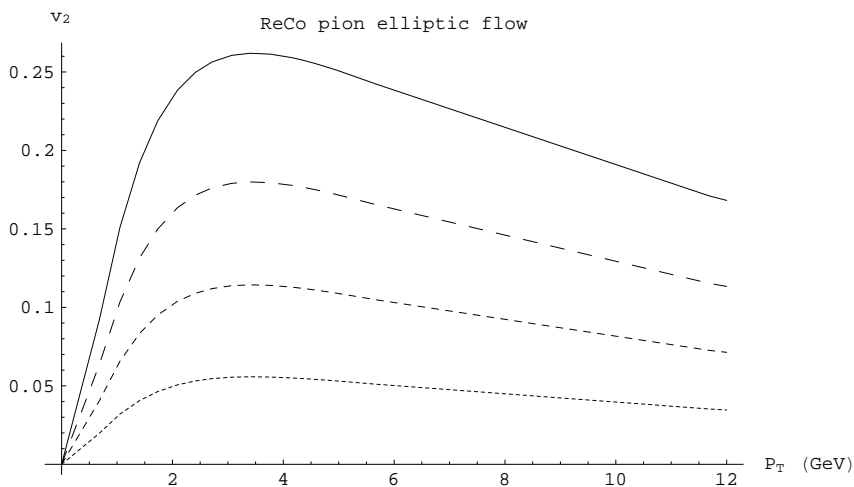


Figure 5.10: The pion elliptic flow at (from top to bottom) $\xi = 0.8$, $\xi = 0.6$, $\xi = 0.4$ and $\xi = 0.2$, assuming a broad amplitude. As in the parton case, a larger impact parameter directly leads to more anisotropy.

5.3.3 Protons

Unfortunately, the fact that the parton elliptic flow (4.2.9) consists of integrations involving Bessel functions, made it necessary for us to use fits to this function in order to be able to

calculate the resulting proton elliptic flow through the multi-dimensional integrals in equation (4.4.17). The proton elliptic flow at $\xi = 0.4$ made in this way, using three different³ fits to the parton elliptic flow, is shown in figure 5.11. We see that the resulting elliptic flow behavior is identical for all three fits, except for a bump at $P_T \approx 0.7$ GeV. It may have to do with the steep slope of the original parton elliptic flow in this transverse momentum regime (see figure 5.8).

Even though all three lines in figure 5.11 have this bump, its size varies strongly, even if we only vary the *size* of the data set that is used to generate the fit! So it is uncertain whether this bump has any physical relevance or whether it is just an artefact of our numerical calculations. Therefore, in the following plots of the proton elliptic flow, we use only one of the fitting methods (i.e., an interpolation function with a relatively large data set) and we show only the results for $P_T > 1$ GeV.

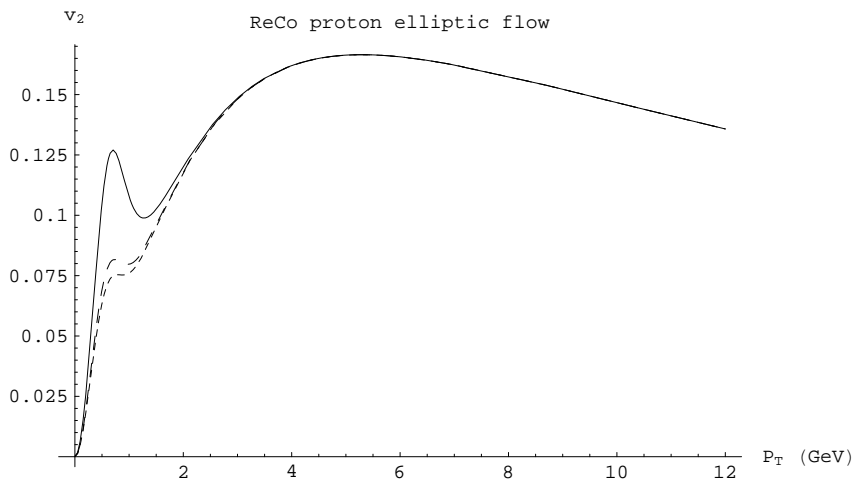


Figure 5.11: The proton elliptic flow at $\xi = 0.4$ with a broad amplitude, resulting from three different fits to the parton elliptic flow: a 47th order polynomial fit (solid line) and two interpolating functions made with a relatively small data set (large dashes) and a large data set (small dashes).

In figure 5.12, we show the (arguably) best broad amplitude proton elliptic flow curve together with the narrow amplitude approximation (4.5.4). As was the case with pions, we see that the peak elliptic flow value is considerably smaller with momentum dispersion (broad amplitude) than it is when the parton momenta are exactly $P_T/3$.

In figure 5.13, the broad amplitude proton elliptic flow is plotted for four values of the impact parameter. As before with partons and pions, we see that for protons the elliptic flow is almost proportional to the impact parameter.

³We do not show a plot containing the three fits and the original parton elliptic flow, because the deviations between the used fits and the original parton elliptic flow are smaller than 0.1%

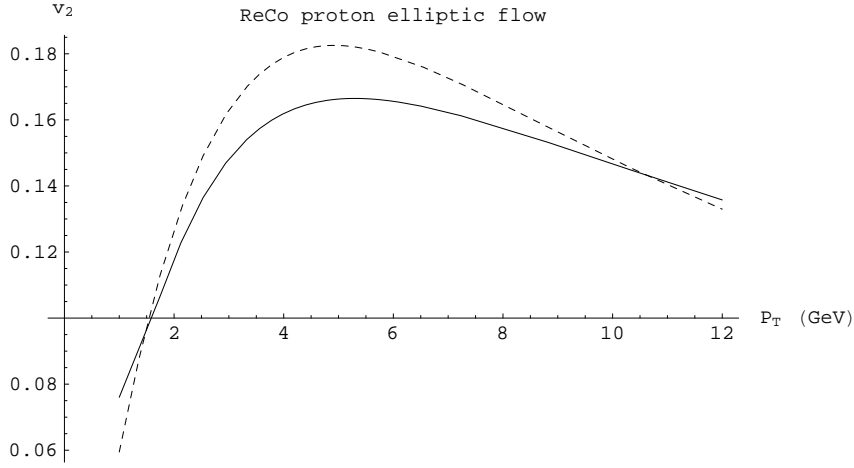


Figure 5.12: The proton elliptic flow at $\xi = 0.4$, resulting from a calculation using a broad amplitude (solid line) and a narrow (delta function) amplitude (dashed line).

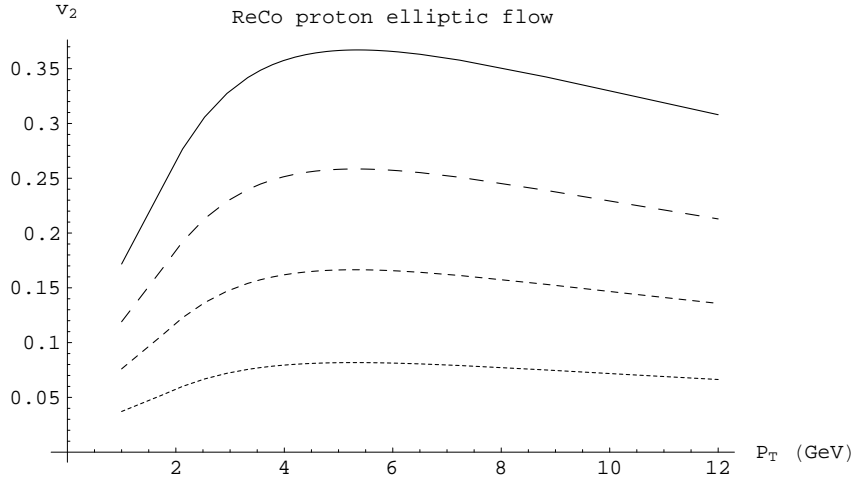


Figure 5.13: The proton elliptic flow at (from top to bottom) $\xi = 0.8$, $\xi = 0.6$, $\xi = 0.4$ and $\xi = 0.2$, assuming a broad amplitude.

5.3.4 Quark number scaling

The most interesting pictures in this chapter are undoubtedly figures 5.14 and 5.15. In these plots, quark number scaling is tested by simply plotting the pion and proton elliptic flows of the previous sections scaled with factors of two and three respectively (see section 4.5). The scaling law (4.5.7) read

$$v_2^h(P_T) = n v_2(P_T/n). \quad (5.3.4)$$

If this law would be exactly obeyed by the pions and protons in our model, the three lines in figure 5.14 and figure 5.15 would completely coincide. But to arrive at (4.5.7) from the general elliptic flow expressions (4.3.17) and (4.4.17), we took two crucial steps:

1. we used the narrow amplitude approximation;
2. we neglected terms that involved the parton v_2 to quadratic and higher order with the argument that the parton elliptic flow is smaller than 0.1 anyway.

Now it is easy to understand from the formulas why we have not found exact quark number scaling in figures 5.14 and 5.15: to arrive at figure 5.14, we used the narrow amplitude approximation, but we did not neglect higher order terms. Therefore, it shows a small violation of the scaling law. With figure 5.15, we took neither of the two steps since we used *broad* amplitudes and all terms in the numerator and dominator of the hadron elliptic flow were taken into account. It should therefore not be surprising that it shows a much larger violation of quark number scaling. Although this prediction of violation of the quark number scaling when using broad amplitudes is not mentioned in Ref. [3], it was recently discussed in Ref. [21]. It is interesting to note that the predicted violation of scaling is largest for protons, not only with realistic broad amplitudes but also in the narrow amplitude approximation. However, all predicted deviations are smaller than 20%.

Actually, it is also intuitively natural that the use of broad amplitudes is linked to violation of quark number scaling. Remember that the use of broad amplitudes simply means that the coalescing quarks are allowed to have different instead of equal momenta, as long as they add up to the hadron momentum. An intuitive way of explaining the measured quark number scaling in terms of recombination processes, would be to paint a picture in which the coalescing quarks each bring in their own elliptic flow and their own transverse momentum $P_T/2$ or $P_T/3$ and consequently the resulting hadron of momentum P_T inherits their elliptic flow behavior. But this is saying that the momenta of the coalescing quarks *are* equal, so we should not be surprised if a picture in which the quark momenta are unequal leads to a violation of this effect.

It is very important to note that one of the main experimental observations that led to the interest in recombination models for the hadronization process in the first place, was the observed quark number scaling (e.g., figure 1.1). However, it now turns out that the recombination model of Ref. [3] does not predict exact quark number scaling if realistic broad longitudinal amplitudes are used. This may weaken the support for this recombination model, and perhaps recombination models in general. It could provide us with a way to falsify this recombination model: if future elliptic flow measurements point to *exact* instead of *approximate* quark number scaling, it would prove that something is wrong with this model.

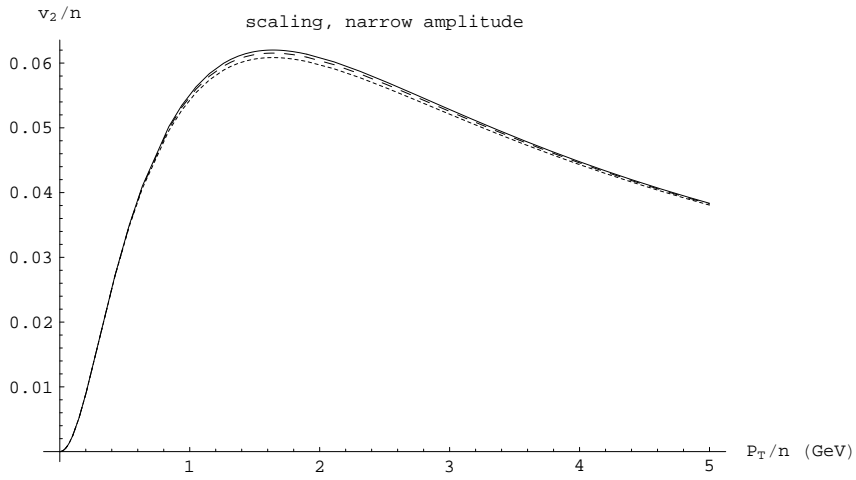


Figure 5.14: The parton elliptic flow (solid line) together with scaled narrow amplitude calculations of the pion (large dashes) and proton (small dashes) elliptic flows.

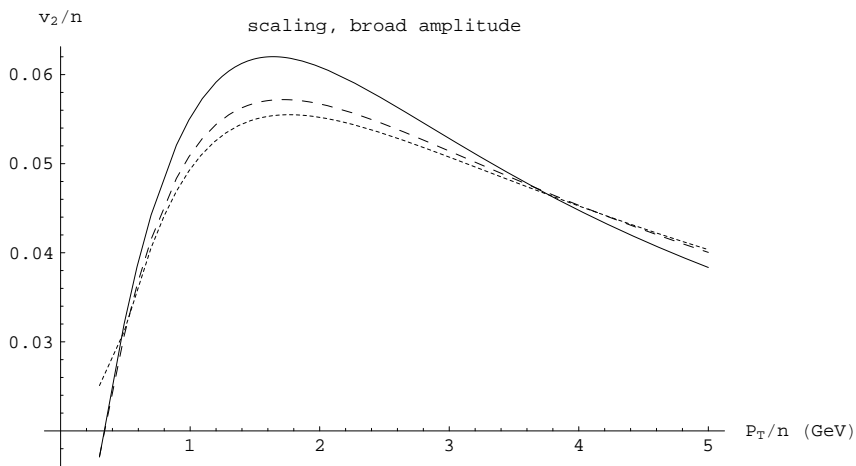


Figure 5.15: The parton elliptic flow (solid line) together with scaled broad amplitude calculations of the pion (large dashes) and proton (small dashes) elliptic flows.

Chapter 6

Conclusions

The hadron spectra and baryon-to-meson ratios that were found in heavy ion collision experiments at RHIC are not in agreement with fragmentation as the dominant hadronization mechanism for transverse hadron momenta smaller than $4 - 6 \text{ GeV}/c$. Moreover, the hadron elliptic flows seem to be linked by quark number scaling, which is not expected in a fragmentation picture either. These disagreements led to the introduction of recombination models, which describe how quarks from a hot and dense phase after the collision, coalesce in a simple way to form hadrons.

We have investigated the recombination model by Fries *et al.* [3]. This recombination model, when combined with fragmentation processes for high transverse momenta, correctly describes the measured hadron spectra. It can also account for the unusually large baryon-to-meson ratios that have been found. However, a realistic recombination model, in which the coalescing quarks are allowed to have different momenta, only predicts *approximate* quark number scaling of the elliptic flow. Deviations stay within 20%, but this feature could weaken the support for recombination models.

Appendix A

Modified Bessel functions

A.1 Modified Bessel functions of the first kind

The most common way to define the so-called modified Bessel functions of the first kind is (for $n \in \mathbb{Z}_{\geq 0}$)

$$I_n(z) := \frac{1}{\pi} \int_0^\pi d\varphi \cos(n\varphi) e^{-z \cos \varphi}. \quad (\text{A.1.1})$$

We can rewrite the right side of this definition in the following way:

$$\begin{aligned} \frac{1}{\pi} \int_0^\pi d\varphi \cos(n\varphi) e^{-z \cos \varphi} &= \frac{1}{\pi} \int_0^\pi d\varphi \cos(n\varphi) e^{+z \cos(\varphi-\pi)} = \frac{1}{\pi} \int_{-\pi}^0 d\xi \cos n(\xi + \pi) e^{z \cos \xi} \\ &= \frac{1}{\pi} \int_{-\pi}^0 d\xi (-1)^n \cos(n\xi) e^{+z \cos \xi} = \frac{1}{\pi} \int_\pi^0 -d\phi (-1)^n \cos(n\phi) e^{z \cos \phi} \\ &= \frac{1}{\pi} \int_0^\pi d\phi (-1)^n \cos(n\phi) e^{z \cos \phi} = \frac{1}{\pi} \frac{1}{2} \int_{-\pi}^\pi d\phi (-1)^n \cos(n\phi) e^{z \cos \phi} \\ &= \frac{1}{2\pi} \int_0^{2\pi} d\phi (-1)^n \cos(n\phi) e^{z \cos \phi}. \end{aligned} \quad (\text{A.1.2})$$

It immediately follows that, for the specific functions I_0 , I_2 , I_4 and I_6 , the resulting alternative (but equivalent) definitions are

$$I_0(z) = \frac{1}{2\pi} \int_0^{2\pi} d\phi e^{z \cos \phi}; \quad (\text{A.1.3})$$

$$I_2(z) = \frac{1}{2\pi} \int_0^{2\pi} d\phi \cos(2\phi) e^{z \cos \phi}; \quad (\text{A.1.4})$$

$$I_4(z) = \frac{1}{2\pi} \int_0^{2\pi} d\phi \cos(4\phi) e^{z \cos \phi}; \quad (\text{A.1.5})$$

$$I_6(z) = \frac{1}{2\pi} \int_0^{2\pi} d\phi \cos(6\phi) e^{z \cos \phi}. \quad (\text{A.1.6})$$

A.2 K_1 , a modified Bessel function of the second kind

The modified Bessel function of the second kind K_1 is usually defined as

$$K_1(z) := \frac{1}{2} z \int_1^\infty d\zeta e^{-z\zeta} \sqrt{\zeta^2 - 1}. \quad (\text{A.2.1})$$

We can rewrite the right side of this definition in the following way:

$$\begin{aligned} \frac{1}{2} z \int_1^\infty d\zeta e^{-z\zeta} \sqrt{\zeta^2 - 1} &= \frac{1}{2} z \int_0^\infty d(\cosh \eta) e^{-z \cosh \eta} \sqrt{\cosh^2 \eta - 1} \\ &= \frac{1}{2} \int_0^\infty d\eta (z \sinh \eta e^{-z \cosh \eta}) \sinh \eta \\ &= \frac{1}{2} \left(-e^{-z \cosh \eta} \sinh \eta \Big|_0^\infty + \int_0^\infty d\eta \cosh \eta e^{-z \cosh \eta} \right) \\ &= \frac{1}{2} \left(0 + \int_0^\infty d\eta \cosh \eta e^{-z \cosh \eta} \right). \end{aligned} \quad (\text{A.2.2})$$

Hence an alternative but equivalent definition of K_1 is

$$K_1(z) = \frac{1}{2} \int_0^\infty d\eta \cosh \eta e^{-z \cosh \eta}. \quad (\text{A.2.3})$$

Acknowledgements

I would like to thank the following people: my thesis supervisor Thomas, for welcoming me to the world of high-energy collisions, for finding time to explain the basic concepts to me, and for bringing me in contact with Rainer Fries; my thesis supervisor Eric, for making much more time for me than originally intended, for clear explanations, and most of all for his encouragement; Rainer Fries, for taking the time to carefully read my derivations and for pointing out an inconsistency in my assumptions; Jaap for spending roughly 1024 hours helping me out with computer stuff; finally, the guys and girl from 301 for lots of useful & useless discussions: Matthieu, Bruce, Sietse, Guus, Manouk, Gijs, Tristan, and Wessel.

Bibliography

- [1] R. J. Fries, J. Phys. G30: S853 (2004), nucl-th/0403036.
- [2] R. J. Fries, B. Müller, C. Nonaka and S. A. Bass, Phys. Rev. Lett. **90**: 202303 (2003), nucl-th/0403036.
- [3] R. J. Fries, B. Müller, C. Nonaka and S. A. Bass, Phys. Rev. C **68**: 044902 (2003), nucl-th/0306027.
- [4] S. S. Adler *et al.* [PHENIX Collaboration], nucl-ex/0305036.
- [5] P. A. M. Dirac: *The Principles of Quantum Mechanics*, Oxford University Press, 1930.
- [6] C.-Y. Wong: *Introduction to High-Energy Heavy-Ion Collisions*, World Scientific, 1994.
- [7] S. Albino, B. A. Kniehl, G. Kramer, submitted to Nucl. Phys. B (2005), hep-ph/0502188.
- [8] R. Scheibl and U. W. Heinz, Phys. Rev. C **59**: 1585 (1999), nucl-th/9809092.
- [9] F. Cooper and G. Frye, Phys. Rev. D **10**: 186 (1974).
- [10] J. D. Bjorken, Phys. Rev. D **27**: 140 (1983).
- [11] L. D. McLerran, Lect. Notes Phys. **538**: 291 (2002), hep-ph/0104285.
- [12] S. Soff, S. A. Bass, M. Bleicher, H. Stöcker, W. Greiner, nucl-th/9903061.
- [13] V. Greco, C. M. Ko and P. Lévai, Phys. Rev. C **68**: 034904 (2003), nucl-th/0305024.
- [14] V. Greco, C. M. Ko, Phys. Rev. C **70**: 024901 (2004), nucl-th/0402020.
- [15] S. Pratt, S. Pal, Nucl. Phys. A749: 268-274 (2005), Phys. Rev. C**71**: 014905 (2005), nucl-th/0409038.
- [16] J.-Y. Ollitrault, Phys. Rev. D **46**: 229 (1992).
- [17] S. S. Adler *et al.* [PHENIX Collaboration], nucl-ex/0305013.
- [18] S. S. Adler *et al.* [PHENIX Collaboration], nucl-ex/0304022.

[19] J. Adams *et al.* [STAR Collaboration], nucl-ex/0409033.

[20] J. H. Chen *et al.*, nucl-th/0504055.

[21] V. Greco and C. M. Ko, nucl-th/0505061.